An overview of artificial intelligence techniques for diagnosis of Schizophrenia based on magnetic resonance imaging modalities: Methods, challenges, and future works

Delaram Sadeghi[a], Afshin Shoeibi[b,*], Navid Ghassemi[b], Parisa Moridian[c], Ali Khadem[d], Roohallah Alizadehsani[e], Mohammad Teshnehlab[d], Juan M. Gorriz[f,g], Fahime Khozeimeh[e], Yu-Dong Zhang[h], Saeid Nahavandi[e,i], U Rajendra Acharya[j,k,l]

[a]*Department of Medical Engineering, Mashhad Branch, Islamic Azad University, Mashhad, Iran.*
[b]*Faculty of Electrical Engineering, FPGA Lab, K. N. Toosi University of Technology, Tehran, Iran.*
[c]*Faculty of Engineering, Science and Research Branch, Islamic Azad University, Tehran, Iran.*
[d]*Department of Biomedical Engineering, Faculty of Electrical Engineering, K. N. Toosi University of Technology, Tehran, Iran.*
[e]*Intelligent for Systems Research and Innovation (IISRI), Deakin University, Victoria 3217, Australia.*
[f]*Department of Signal Theory, Networking and Communications, Universidad de Granada, Spain.*
[g]*Department of Psychiatry. University of Cambridge, UK.*
[h]*Department of Informatics, University of Leicester, Leicester, UK.*
[i]*Harvard Paulson School of Engineering and Applied Sciences, Harvard University, Allston, MA 02134 USA.*
[j]*Ngee Ann Polytechnic, Singapore 599489, Singapore.*
[k]*Dept. of Biomedical Informatics and Medical Engineering, Asia University, Taichung, Taiwan.*
[l]*Dept. of Biomedical Engineering, School of Science and Technology, Singapore University of Social Sciences, Singapore.*

Abstract

Schizophrenia (SZ) is a mental disorder that typically emerges in late adolescence or early adulthood. It reduces the life expectancy of patients by 15 years. Abnormal behavior, perception of emotions, social relationships, and reality perception are among its most significant symptoms. Past studies have revealed that SZ affects the temporal and anterior lobes of hippocampus regions

---

*Corresponding author
Email address:* `afshin.shoeibi@gmail.com` (Afshin Shoeibi)

of the brain. Also, increased volume of cerebrospinal fluid (CSF) and decreased volume of white and gray matter can be observed due to this disease. Magnetic resonance imaging (MRI) is the popular neuroimaging technique used to explore structural/functional brain abnormalities in SZ disorder, owing to its high spatial resolution. Various artificial intelligence (AI) techniques have been employed with advanced image/signal processing methods to accurately diagnose SZ. This paper presents a comprehensive overview of studies conducted on the automated diagnosis of SZ using MRI modalities. First, an AI-based computer aided-diagnosis system (CADS) for SZ diagnosis and its relevant sections are presented. Then, this section introduces the most important conventional machine learning (ML) and deep learning (DL) techniques in the diagnosis of diagnosing SZ. A comprehensive comparison is also made between ML and DL studies in the discussion section. In the following, the most important challenges in diagnosing SZ are addressed. Future works in diagnosing SZ using AI techniques and MRI modalities are recommended in another section. Results, conclusion, and research findings are also presented at the end.

1. Introduction

Schizophrenia (SZ) is the most severe psychological disease, which causes devastating effects on the brain and daily activities of the patient [1]. It causes abnormalities in the initial brain growth which may bring about different symptoms such as hallucination, disorder, motivational and cognitive problems [2]. The cause of this neural disorder is unknown, but neuroscientists believe that the interaction between genes and several environmental factors may be the main cause [2, 3]. Taking medicine reduces the psychological symptoms of SZ to some extent. However, these medicines do not improve the social and occupational activities of the patients completely [4]. According to the World Health Organization (WHO) reports, about 21 million individuals around the world

suffer from this disorder. The average age for the onset of this disorder is 18 and 25 years in women and men, respectively with a higher prevalence rate in men [5, 6]. The regions showing the spread of SZ people around the world is illustrated in Fig. 1 [7].
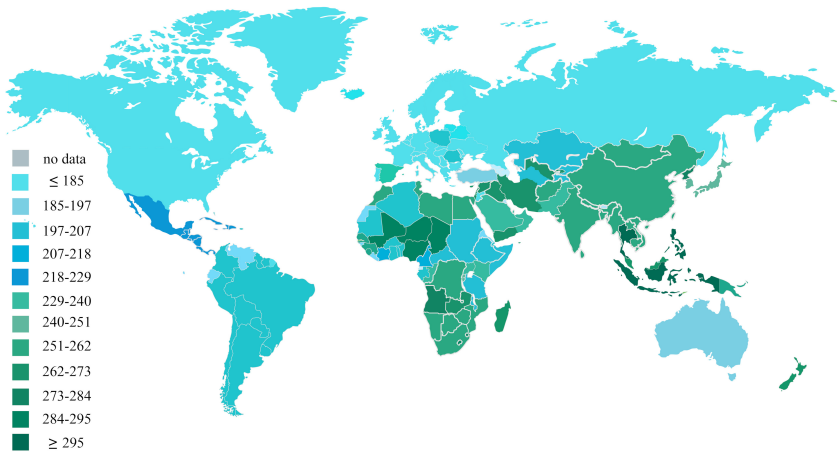

Figure 1: Regions showing the spread of SZ people around the world [7]

Diagnosis of SZ is a challenging problem due to the heterogeneity of this mental disorder and lack of specific effective biomarkers [8]. In order to diagnose SZ, few clinical symptoms including physical, psychiatric, and psychological indicators need to be evaluated [9, 10, 11]. Clinical examination includes various tests such as blood tests as well as medical imaging [12, 13]. If the physicians do not find a physical cause for the suspected symptoms of SZ, they may refer the patient to a psychiatrist, psychologist, or other related experts. The main psychological assessment focuses on clinical interviews based on diagnostic and statistical manual (DSM-IV) of mental disorders conducted by clinical psychiatrists to diagnose patients with SZ [14, 15].

Functional and structural neuroimaging techniques are another important category of methods capable to diagnose SZ [16, 17]. Structural neuroimaging modalities mainly include two methods of structural magnetic resonance imag-

ing (sMRI) [18, 19, 20] and diffusion tensor imaging (DTI) [21, 22], which show the structure of human brain and its structural connectivities, respectively, owing to their high spatial resolution. Overall, MRI based structural neuroimaging modalities are suitable for visualizing white matter (WM), gray matter (GM), and CSF tissues of the brain as well as exploring their abnormalities [23, 24].

Functional neuroimaging modalities for the diagnosis of SZ include electroencephalography (EEG) [25], magnetoencephalography (MEG) [26], functional near-infrared spectroscopy (fNIRS) [27, 28], and functional MRI (fMRI) [29, 30]. High cost and insufficient accuracy have limited the use of MEG and fNIRS for the diagnosis of SZ, respectively.

The EEG is a noninvasive technique used to record the electrical activity of brain by using electrodes placed on the scalp [31, 32]. One of the problems with EEG is finding the exact location of brain activity sources [33, 34].

The fMRI modality is one of the most studied techniques for diagnosing SZ and has two types of resting state (rs-fMRI) [35, 36] and task-based (T-fMRI) [37, 38]. The fMRI does not directly measure neural activity, but measures changes in blood oxygen, volume, and flow [35, 36, 37, 38]. During brain activities, regions of the brain involved in activity have higher blood flow than the rest, which increases oxygen levels [35, 36, 37, 38]. The better spatial resolution of fMRI over EEG and other functional modalities is one of the most important benefits which helps to determine nearly 1mm resolution where an activity occurs in the brain [39, 40].

The limitations of sMRI and fMRI modalities are as follows. The common challenges of these two techniques the presence of noises and artifacts in the images. Hence, there is a need for stillness when recording the images to avoid high motion artifacts [41, 42]. Also, in fMRI, the temporal resolution is relatively low due to the slow hemodynamic response and also more time is needed to record a large volume of images [43, 44]. Hence, it is unable to monitor brain activities in real time [42, 43, 44]. These challenges make it difficult for physicians to accurately diagnose SZ.

Nowadays, computer aided diagnosis systems (CADS) have been proposed

using advanced image processing and AI techniques to help the physicians to automatically diagnose SZ accurately [45, 46, 47]. Conventional machine learning (ML) and deep learning (DL) have been employed to develop highly accurate and robust CADS [48]. In this study, an extensive review is conducted on the diagnosis of SZ using functional and structural modalities of MRI and AI algorithms.

The structure of this paper is as follows. Our search strategy is presented in Section 2. Then, in Section 3, the CADS for diagnosis of SZ based on MRI neuroimaging modalities is introduced and the related papers are reviewed. The main findings are discussed in Section 4. Subsequently, challenges in diagnosing SZ using AI techniques are discussed in Section 5. Finally, the paper is concluded and some future works are proposed in Section 6.

2. Our Search Strategy

In this work, the most important citation databases such as IEEE Xplore, ScienceDirect, SpringerLink, and Wiley have been chosen to search articles on schizophrenia mental disorder. Also, the keywords "Schizophrenia", "sMRI", "fMRI", "Machine Learning", "Artificial Intelligence", and "Deep Learning" are employed in Google Scholar to find the relevant articles. The examination of the latest accepted papers until October 20th, 2020 has been in this article. Figure 2 shows the number of papers published each year after 2016 on the automated detection of SZ using ML and DL techniques. It can be noted from this figure that, Elsevier has published more number of papers as compared to the other publishers.

3. CADS for Schizophrenia Diagnosis Based on Artificial Intelligence Methods

Nowadays, CADS is developed by the researchers to diagnose a variety of brain disorders such as epilepsy [49, 50], autism spectrum disorders (ASD) [51, 52], attention-deficit hyperactivity disorder (ADHD) [53, 54] and SZ [55, 56,

5
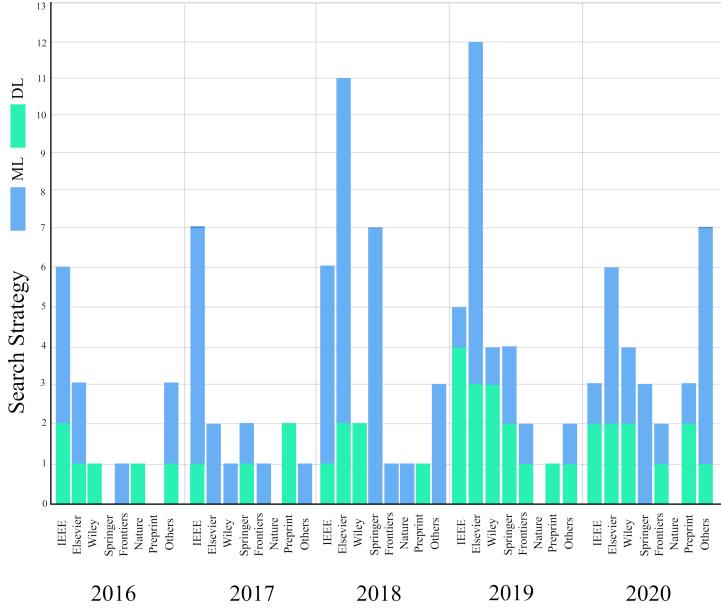
Figure 2: Number of papers published each year since 2016 on automated detection of SZ.

57] using MRI modalities. The implementation of CADS to diagnose SZ uses conventional ML or DL methods. These two categories of AI methods are graphically described in Figure 3.

Figure 3 describes the ML methods for diagnosing SZ, in which the proper selection of feature extraction and feature selection methods requires extensive knowledge of image processing, feature engineering and AI. Also, the CADS steps for DL-based diagnosis of SZ are shown in Figure 3. It can be seen that in DL, feature extraction and reduction/selection steps are merged into an automatic feature extraction step. Needing little knowledge of the field, intelligent and automatic representation learning, and good performance on big data are among the most important advantages of DL over ML. The important subsections of CADS for the automated diagnosis of SZ are presented in Figure 3.
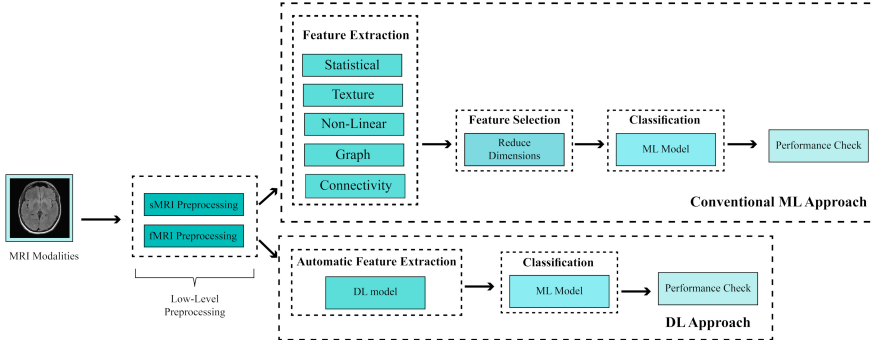
Figure 3: Illustration of automated diagnosis SZ using of AI techniques.

3.1. Available Datasets

In this section, the freely available sMRI and fMRI neuroimaging datasets used for the diagnosis of SZ are introduced. Schizconnect [58], NUSDAST [59], COBRE [60], FBIRN [61], MCIC [62], UCLA [63], MLSP 2014 [64] are the important publicly available datasets for SZ detection. The details of these datasets are given below.

3.1.1. Schizconnect

This dataset has 1392 subjects used to diagnose SZ. In this dataset, 632 people have an undiagnosed disease, 215 people have broad SZ, 384 people have strict SZ, 41 people have schizoaffective disorder, 10 people have bipolar disorder, 44 people have sibling of SZ strict and 66 people have sibling of no known disorder [58].

3.1.2. NUSDAST

This dataset can be downloaded as part of the SchizConnect dataset site. It contains various neuroimaging data obtained from 450 people with SZ, healthy controls, and their siblings over 2 years. Neuroimaging data includes sMRI, landmarks maps, FreeSurfer measurement, and segmentation. Cognitive data includes scores for crystallized intelligence, working memory, episodic memory, and executive performance. Clinical data includes demographics, sibling

7

relationships, SAPS and SANS psychopathology. Genetic data is also 20 single nucleotide polymorphisms (SNPs). In addition to this dataset, CAWorks neuroimaging analysis software is also available. More information about this dataset is provided in [59].

3.1.3. COBRE

A variety of neuroimaging modalities including rs-fMRI, sMRI, and phenotype and other diagnostic information from 72 patients with SZ and 75 healthy individuals (age range 18-65 years in each group) are included in this dataset. More information is provided in [60].

3.1.4. FBIRN

It has three phases, with only second and third phases contain the data on people with SZ. Phase II consists of 87 individuals with DSM-IV SZ or schizoaffective disorder and 85 healthy individuals aged between 18-70 years. This dataset has sMRI of T1-weighted and T2-weighted contrasts. In addition, the third phase dataset includes neuroimaging modalities of DTI, sMRI, fMRI, and behavioral data, as well as clinical and demographic evaluations of 186 healthy individuals and 176 schizophrenics obtained from the United States [61].

3.1.5. MCIC

This multi-site dataset contains a variety of sMRI, DTI, and fMRI neuroimaging modalities; all of which were obtained from 162 SZ patients and 169 healthy individuals. Clinical and cognitive assessments, genetic testing, etc. are also listed in this dataset. This dataset is available to the public through COINS [62].

3.1.6. UCLA

This dataset contains various neuroimaging modalities including T-fMRI, rs-fMRI, sMRI, and diffusion-weighted imaging (DWI), as well as phenotype information obtained from 130 healthy individuals, 50 subjects with SZ, 49

subjects with bipolar disorder, and 43 subjects with ADHD. The description about the types of tasks for recording T-fMRI and preprocessing steps performed on images can be obtained from [63].

3.1.7. MLSP 2014 Schizophrenia Classification Challenge

The MLSP dataset was introduced in a challenge held in 2014 under the auspices of the IEEE. This data contains sMRI and fMRI modalities recorded from 75 healthy individuals and 69 patients with SZ [64]. More detailed information about the dataset is given in Table 1.

Table 1: Details of freely available public MRI datasets used for automated detection of SZ.

Dataset	Publisher	Modalities	Number of Cases	Link
SchizConnect	SchizConnect	sMRI, fMRI	No Known Disorder=632 Schizophrenia Broad=215 Schizophrenia Strict=384 Schizoaffective=41 Bipolar Disorder=10 Sibling of Schizophrenia Strict=44 Sibling of No Known Disorder=66	http://www.schizconnect.org/
COBRE	–	rs-fMRI, Anatomical MRI	Schizophrenia=72, Healthy=75	http://fcon_1000.projects.nitrc.org/indi/retro/cobre.html https://data.mendeley.com/datasets/3h4mt7xryk/1
NUSDAST	NIH-Funded Data Sharing Project	sMRI	Schizophrenia=171, Healthy=170 Non-Psychotic Siblings=44 Healthy Siblings=66	https://central.xnat.org/app/action/DisplayItemAction/search_value/ NUDataSharing/search_element/xnat:projectData/search_field/xnat: projectData.ID
FBIRN Phase II FBIRN Phase III	The Function Biomedical Informatics Research Network	fMRI	Schizophrenia=87, Healthy=85 Schizophrenia=87, Healthy=85	https://www.nitrc.org/projects/fbirn/ https://www.nitrc.org/projects/mcic/ https://coins.trendscenter.org/
MCIC	–	sMRI, fMRI, DWI	Schizophrenia=162, Healthy=169	https://openneuro.org/datasets/ds000115/versions/00001
UCLA	UCLA Consortium for Neuropsychiatric Phenomics	fMRI, sMRI, DWI	Schizophrenia=50, Bipolar Disorder=49 ADHD=43, Healthy=130	https://openneuro.org/datasets/ds000030/versions/1.0.0
MLSP 2014	IEEE	fMRI, sMRI	Schizophrenia=69, Healthy=75	https://www.kaggle.com/c/mlsp-2014-mri

3.2. Preprocessing for sMRI and fMRI Modalities

In this section, the most important low-level preprocessing techniques of sMRI and fMRI modalities are reviewed. The sMRI and fMRI neuroimaging modalities are usually very complex, difficult, and time consuming to analyze. In addition, one of the most important problems with MRI-based data is the presence of various artifacts which always pose a serious challenge to physicians and radiologists in accurately diagnosing the type of disease. Therefore,

if appropriate methods are not used for preprocessing while analyzing MRI-based images, the diagnosis of brain diseases may be erroneous. To solve these problems, various software packages have been introduced in recent years to pre-process sMRI and fMRI modalities, the most important of which are FMRIB Software Library (FSL) [65], brain extraction tools (BET) [66], FreeSurfer [67] and SPM [68]. In the following sections, the important low-level preprocessing techniques for sMRI and fMRI neuroimaging modalities are discussed.

3.2.1. Standard (Low-level) sMRI preprocessing steps

Conventional preprocessing methods for sMRI images are introduced in this section. Important preprocessing steps for this data type include denoising, inhomogeneity correction, skull stripping, registration, intensity standardization, de-oblique, re-orientation, and segmentation [69, 70, 71]. They are briefly explained below.

1. **Denoising:** The sMRI images are exposed to various noises during the recording process [69, 70, 71]. Classic filters [72, 73], wavelet filters [74], etc. are among the most common methods of noise removal in sMRI imaging [69, 70, 71].

2. **Inhomogeneity Correction:** The resulting defect in the coils of MRI scanner is seen as a low frequency change in signal intensity of sMRI images. Rectifying this artifact should be performed before any quantitative sMRI analysis [69, 70, 71].

3. **Skull-Stripping:** During sMRI imaging, brain and skull tissues are recorded. But the skull does not contain important information for processing. Therefore, when analyzing sMRI images, this part is removed by various methods [69, 70, 71].

4. **Registration:** In sMRI analysis, this stage of preprocessing is very common for merging different types of image modalities and sequences; also it can be used for transforming images into a common standard space such as MNI [69, 70, 71].

5. **Intensity standardization:** The sMRI obtained from different scanners will not have the same exact intensity, even if those scanners followed the same imaging protocol. Intensity standardization techniques attempt to correct these changes by a scanner-dependent manner [69, 70, 71]. Histogram matching techniques are the most commonly used technique for MRI intensity standardization [69, 70, 71].

6. **De-Oblique:** During the sMRI recording process, the scan angle sometimes deviates from horizon to record the entire brain which is called the oblique scan. In such circumstances, data registration may be done with less noise, but it makes registration between different images difficult. Therefore, in some studies, de-oblique preprocessing is performed [69, 70, 71].

7. **Re-orientation:** It specifies the image orientation process settings. Differences in image orientation can lead to mis-registration. As such, images are transformed and re-oriented to have the same direction [69, 70, 71].

8. **Segmentation:** Segmentation of sMRI image divides it into different brain textures, including white matter, gray matter, and CSF or into distinct brain regions. Segmentation can be used for a variety of purposes. For example, segmentation for the normalization process or using a specific segmentation to generate a mask for a region of interest (ROI) [69, 70, 71].

3.2.2. Standard (Low-level) fMRI preprocessing steps

Important fMRI preprocessing techniques include removal of first N volumes, slice timing correction, motion correction and volume scrubbing, normalization, spatial smoothing, and temporal filtering [75, 76, 77], each of which is described below.

1. **Removal of the First N Volumes:** When a magnetic field is applied to the brain, the hydrogen spins orient themselves in the direction of the magnetic field, and it takes about 5 to 6 seconds for these spins to reach a steady state. Therefore, the volume images obtained in the first few seconds should be deleted to balance the signal and also let the patient

11

get used to the device environment to reduce the artifacts of recorded fMRI data [75, 76, 77].

2. **Slice Timing Correction:** This step aims to make blood oxygenation level dependent (BOLD) time series of all voxels located in different slices to have the same reference time which is usually the acquisition time of the first slice [75, 76, 77].

3. **Motion Correction and Volume Scrubbing:** Motion correction is used to correct head movements during fMRI recording. Motion correction by aligning the data with a reference image tries to minimize the effect of movements on the data. This reference is usually the first volume. In the next step, an approach called volume scrubbing is performed, which means removing images that have very intense head movement artifacts [75, 76, 77].

4. **Normalization:** The size, shape, and anatomy of the brain vary from person to person, so inter-subject comparisons are necessary to allow images to be transferred to a standard template, or in other words to be spatially normalized. Currently, the most popular template is the MNI, however other templates are also available [75, 76, 77].

5. **Spatial Smoothing:** It involves a weighted averaging of BOLD signals of adjacent voxels. This process is persuasive on account of neighboring brain voxels being usually highly correlated in function and blood supply [75, 76, 77].

6. **Temporal Filtering:** In fMRI modality, the important information lies in the frequency band lower than 0.1 Hz. However, the components lower than 0.01 Hz are known to be slow drift of non-neural origin. Therefore, a band-pass filter with a frequency band of 0.009-0.08 Hz is usually used to remove undesired components [75, 76, 77].

3.3. Artificial Intelligence Methods

As mentioned in the previous sections, AI methods include two important categories of ML and DL techniques. The AI methods are used to automati-

12

cally detect SZ in this section. First conventional ML methods and then DL techniques are discussed.

3.3.1. Conventional Machine Learning Methods

The most important difference between CADS based on DL and conventional ML according to Figure 3 is in the blocks of feature extraction and feature selection. In this section, the most important steps of feature extraction and feature selection for the automated diagnosis of SZ are described in Table 2. Tables 2 and 3 show that diagnosis of SZ by conventional ML methods has been of more interest to researchers than by DL. The main reasons behind the popularity of traditional ML over DL are; (i) ML methods are still relatively common and widespread, (ii) works well with even a small dataset. The description of the CADS sections based on ML methods are given below.

Feature Extraction Techniques Feature extraction is the most important part of ML technique based diagnosis of SZ. It can be noted from Table 2 that the most important feature extraction techniques employed for SZ detection using MRI modalities are statistical, textural, nonlinear, graph, and connectivity matrix.

1. **Statistical:** Statistical moments are considered as the most basic feature extraction techniques, which include mean, variance, standard deviation, moments, and so on [78, 79]. Authors in [80, 81], have used these methods to extract these features.

2. **Texture:** Textural features are the important feature extraction technique used in medical images [82, 83]. Using these methods, important informations are extracted from the texture of images. Grey level co-occurrence matrices (GLCM)-based methods [84, 85], and Gabor filters [86, 87] are the most important texture methods. Authors in [88, 89] have proposed a method to diagnose SZ based on textural features.

3. **Non-Linear:** Extracting nonlinear features from neuroimaging modalities is very useful and may increase the performance of SZ diagnosis [90]. In research [91], authors used non-linear features for SZ detection.

13

4. **Graph:** Another group of features used for the diagnosis of SZ is based on graph models. In these methods, a graph is first constructed or extracted from the data in an innovative way. Then, with the help of graph and local graph properties, the data is displayed again. These methods can also be used to select an unsupervised feature [92, 93]. A number of studies have used graph-based features to diagnose SZ [94, 95].

5. **Connectivity Matrix:** Connectivity matrix feature extraction methods are the primary scheme of feature extraction used for processing DTI and fMRI neuroimaging modalities [96, 97]. These features provide an informative representation about the structure and function of brain. Functional connectivity matrix (FCM) [98, 99] and structural connectivity matrix (SCM) [100] are the methods used for fMRI and DTI modalities, respectively. In several works, the FCM technique are used to features from MRI images to detect SZ.

Feature Reduction / Selection Methods

Choosing the right feature selection method when designing CADS improves the diagnosis performance of SZ. In addition, when the size of the data attribute space is very large, using an appropriate feature set helps to reduce the computational costs required to train the system. So far, several methods have been proposed for feature reduction or feature selection problems [101, 102, 103]. The important feature reduction and selection methods used in CADS systems for SZ diagnosis are discussed below.

- **Feature Reduction Techniques:** In these methods, the feature matrix is first received and then is transferred from the input space to an output space of reduced dimension. In few studies, principal component analysis (PCA) technique has been used to reduce features and improve the specificity [104].

- **Feature Selection Methods:** In these methods, an optimum subset of basic features is selected and used. Feature selection algorithms are

divided into three types: (i) supervised [105], (ii) unsupervised [106], and (iii) optimization [107]. They are briefly discussed below.

Supervised Feature Selection Methods

Methods for selecting supervised features include techniques based on Relief [108], Fisher [109], Chi-Squared [110], and correlation [111] types. The details of these methods are given below.

1. **Relief Feature Selection:** In this method, at each step, a sample is randomly selected from the samples in the dataset. Then, the degree of relevance of each attribute is updated based on the difference between the selected sample and two neighboring samples [108]. If one of the features of the selected sample differs from the similar feature in the neighboring samples of the same class, the score of this feature is reduced. On the other hand, if the same feature in the selected sample differs from the similar feature in the neighboring samples of the opposite class, the score of this feature increases [108]. Authors in [112], have used relief algorithms to select the features.

2. **Fisher Feature Selection:** This technique selects attributes that minimize inter-class distances between samples, while maximizing the distance for intra-class ones; also, this method is often used for binary classification problems [49, 109]. Through this method, the importance (weight) of each feature is determined. In [113], Fisher selection method is used to select the features.

3. **Chi-Squared Feature Selection:** Working based on the chi-square test [110], this method tries to find features that have a relation with the input data (I.e., they are dependant). In order to be able to properly use this test to measure the relationship between various features in a data set and the target attribute, there must be two conditions for attribute attribution and independent sampling of attributes [110]. Authors in [114, 115] have used this method to select the features in CADS for the diagnosis of SZ.

4. **Correlation Based Feature Selection:** Correlation-based techniques

are the supervised feature selection methods, few of such methods have also been used in CADS to diagnose SZ [111]. Correlation-based techniques have shown excellent performance for feature selection.

Unsupervised Feature Selection Methods

The methods of variance, mean absolute value of the differences, scatter ratio, Laplacein score, and finally the clustering are the important unsupervised feature selection methods used [116, 117, 118, 119]. In [120], agglomerative hierarchical clustering feature selection method is used to diagnose SZ. In another study, authors in [91] tested the fuzzy rough set method and achieved promising results.

Feature Selection Based Optimization Methods

It is the another class of feature selection techniques used in the diagnosis of SZ. Genetic algorithms (GA) [121, 122], ant colony optimization (ACO) [123], binary particle swarm optimization (BPSO) [124] and non-dominated sorting genetic algorithm II (NSGA-II) [125] have been used in various studies to select the features for the diagnosis of SZ.

3.3.2. Deep Learning Methods

DL is an emerging field which is widely used in neuroscience for the automated diagnosis of mental disorders such as bipolar disorder [126, 127], personality disorders [128], depression [129], and schizophrenia [130]. In order to diagnose SZ using sfMRI and fMRI neuroimaging modalities, DL techniques have been used. As shown in Table 2, most of the researches have focused on implementing various convolutional neural network (CNN) models to diagnose SZ. The reason for this choice is the excellent performance of CNNs using 2D and 3D data [131, 132, 133]. However, research has shown that these networks also performed very well on one-dimensional medical data. Autoencoders (AEs) [134, 135], recurrent neural networks (RNNs) [134, 135], deep belief networks (DBNs) [134, 135], generative adversarial networks (GANs) [136], CNN-AE [134, 135], and CNN-RNN networks [134, 135] have also been used in few studies. They are briefly explained in the following subsections.

16

Convolutional Neural Networks (CNNs)

CNNs have been used for automated diagnosis of SZ, which includes 1D-CNN, 2D-CNNs, Inception, GANs, CapsNet, and finally 3D-CNN. The details of these models are given below.

1. **1D and 2D CNN:** The computer vision and image processing have drawn the attention of many researchers' since 1960s [134, 135, 137]. Nevertheless, given the high dimensionality of images, image processing tasks, such as classification and segmentation, have always been considered as difficult tasks. In 2012, AlexNet, which is a form of deep neural networks with 2D convolutional layers is able to reach high accuracies for image classification tasks [134, 135]. Since then, many other models have been presented, aiming to improve the performance of prior ones, such as VGG [138, 139], GoogleNet [140]. Also, other variations of 2D-CNN have been created to make them suitable for other data types such as 1D-CNN, which is more suitable for electroencephalogram (EEG) [141]. Figure 4 shows a sample 2D-CNN architecture used for automated detection of SZ using MRI modalities.
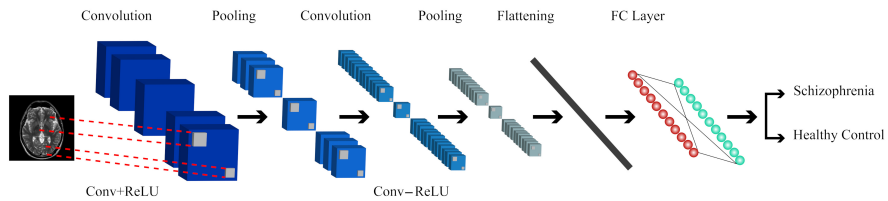

Figure 4: Block diagram of 2D-CNN used for automated SZ detection.

2. **Inception:** In the year 2014, two important network structures VGG and GoogLeNet are introduced. GoogLeNet, the winner of ImageNet challenge, had two primary ideas to overcome the vanishing gradient issue and go deeper [134, 135]. The first idea in this network is to use gradient injection, i.e., using a middle-level output for back-propagation additional

17

to the last layer's output. The second and more important one is the inception layer. Inception layers combine the filters of various sizes to detect patterns of different lengths in the data. However, they also apply a 1x1 filter at the end of these blocks to reduce the number of parameters. Inception blocks are combined with many other structures to form more complicated and robust models, such as Inception-ResNet [142].

3. **Generative Adversarial Networks (GANs):** Generative models are not merely attractive due to their ability to generate new samples, but also the idea of making an algorithm that can generate samples itself is a significant step in creating intelligent models. However, the primary use of these models in biomedical data processing is to increase the size of datasets. Before GANs, many other generative models have been introduced. However, the quality of generated data samples is a concern in those models. Generative adversarial nets [136, 143] are first introduced mainly for images, and many other models have been created for other data types also [136, 143]. In addition to generating new data, GANs can be used as unsupervised learning models as well [136, 143, 144]. Figure 5 shows a sample GAN architecture used for automated detection of SZ using MRI modalities.
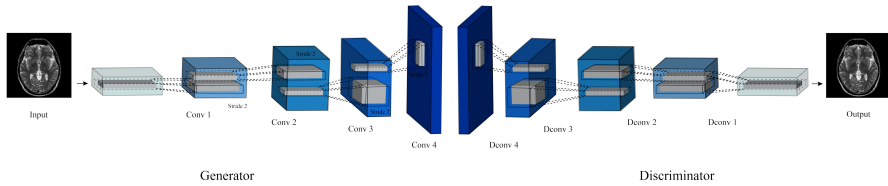

Figure 5: Block diagram of GAN used for automated detection of SZ.

4. **CapsNet:** The most important milestone in creating deep neural networks is to make them generalizable [134, 135]. Nowadays, many researchers try to do so by creating big datasets which contain various samples to include different situations that the data sample can be presented

in; however, the CNNs' underperformance in the presence of data with a different orientation than training data stays as the primary deficiency of these models. CapsNet tried to address this issue by creating a network that implicitly performs reverse graphics [145, 146]. To achieve this, CapsNet proposed a block, capsule, which tries to determine the presence of an object in a given location and its instantiation. In recent years CapsNets have shown state-of-the-art performances in many applications [145, 146]. Figure 6 shows a sample CapsNet architecture used for automated detection of SZ using MRI modalities.
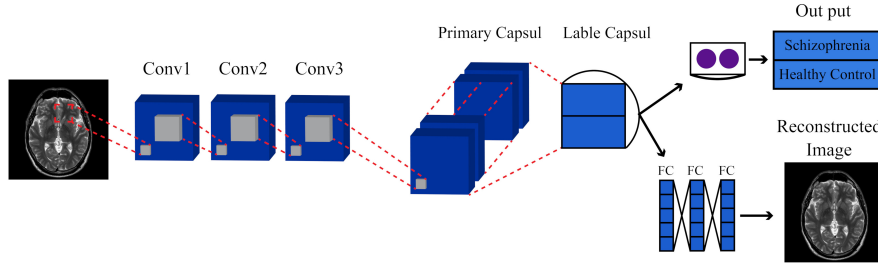

Figure 6: Block diagram of CapsNet used for automated detection of SZ.

5. **3D-CNN:** Convolutional neural nets perform well for 2D and 1D data due to their lower number of trainable parameters and transfer learning. However, for 3D datasets, designing and training a neural net is not as easy, considering the low volume of 3D datasets and a large number of trainable weights. Nevertheless, the possibility of finding spatial 3D patterns in the data has intrigued researchers to try to design and train 3D-CNNs despite their limitations [134, 135]. There are many 3D-CNNs have been developed to reach state-of-the-art performances [147, 148]. Figure 7 illustrates a sample 3D-CNN architecture used for automated SZ using MRI modalities.

Recurrent Neural Networks (RNNs)

Time-series and sequential data form a significant part of the data types.

19
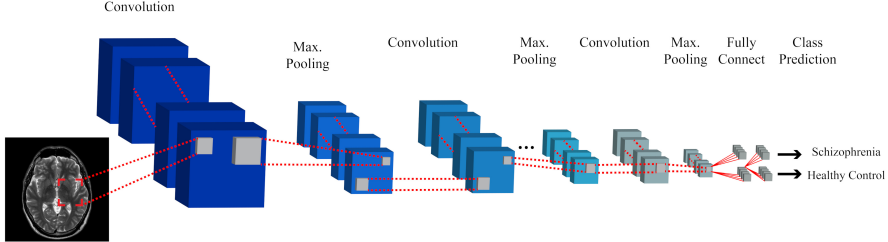
Figure 7: Block diagram of 3D-CNN used for automated SZ detection.

Recognizing temporal patterns while processing these data play a key role. However, the previous models developed are capable of recognizing spatial patterns, but they are not suitable for recognizing temporal patterns. Hence, recurrent neural nets (RNNs) are proposed to address this issue, which is a particular form of neural nets that can be scaled to detect distant patterns in time-series [134, 135]. Long short term memory (LSTM) and gated recurrent units (GRU) are the two famous building blocks of RNNs [134, 135].

Autoencoders (AEs)

Unsupervised learning is an exciting field in ML as it can eliminate all the overheads of feature engineering. Hence, AEs has been developed and used in many recent works [134, 135]. Basically, AEs try to map data to a smaller latent space by minimizing the loss function and then back to the original space [134, 135]. This moves the AEs toward preserving important characters of data while reducing its dimensionality. In recent years, many variants of AEs have been presented to improve their performance, such as stacked AE [149], denoising AE [150], and sparse AE [151]. Figure 8 illustrates a sample AE architecture used for automated detection of SZ using MRI modalities.

Deep Belief Networks (DBNs)

Deep belief networks are a group of generative models created based on graphical models. These networks are composed of multiple layers of latent variables, and they have connections between layers but not within layers themselves. While they are considered as one of the premiers of the new era of DL

20
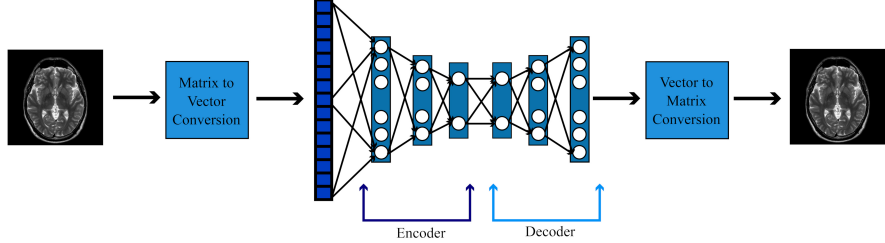
Figure 8: Block diagram of an AE used for automated SZ detection.

and have been around for more than a decade [134, 135], nevertheless, they are still widely used in recent studies with state-of-the-art performances.

CNN-AE

In order to use the benefits of convolutional layers in AEs for unsupervised representation learning, convolutional AEs (CNN-AEs), are introduced [49]. Figure 9 illustrates a sample CNN-AE Architecture used for automated detection of SZ using MRI modalities. Due to the large number of learnable parameters, regular AEs usually overfit when fed with raw data, and they will not learn anything useful. So, applying convolutional layers can help to reduce the number of learnable parameters, and hence will make the network to adequately train. A combination of this model with others, such as sparse AE, can help to yield higher performance [134, 135, 49].
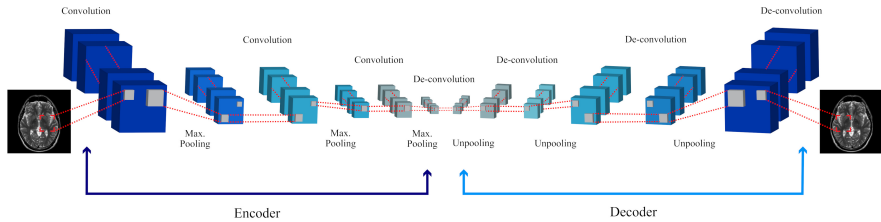

Figure 9: Block diagram of CNN-AE used for automated SZ detection.

CNN-RNN

While RNNs are strong in finding temporal patterns, they have issues when

21

faced with spatial patterns [134, 135]. CNNs are the opposite, so if appropriately combined, a robust network capable of processing data with various types of characteristics, such as biomedical signals, can be created. Nowadays, CNN-RNNs are commonly used for signal processing tasks [152, 153]. In these networks, first few layers of convolution process data and extract features; then, these features are fed to RNN layers to make the final decision on the input [134, 135]. Figure 10 illustrates the CNN-RNN network used for automated SZ detection. In this figure, many improvements can be made to this network, such as feature fusion to obtain higher performances [134, 135].
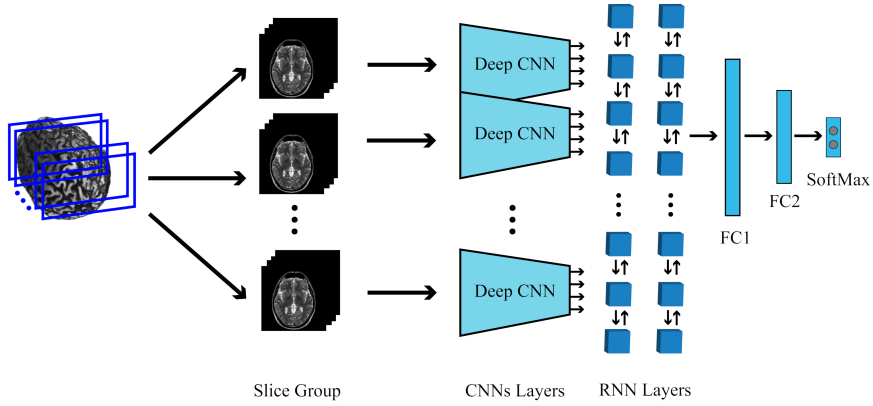
Figure 10: Block diagram of CNN-RNN used for automated SZ detection.

3.3.3. Classification Methods

The classification is the last part of CADS used to automatically detect SZ in DL. The support vector machines (SVM) [154, 155], random forest (RF) [156] and Softmax [157] are among the widely used classification methods in the diagnosis of schizophrenia. Among the mentioned methods, Softmax method is used only in DL applications. On the other hand, SVM and RF classification techniques are used in both types of CADS, but the technique of implementing these methods is different in DL implementations [134, 135]. Details of the

22

CADS implementation based on DL and conventional ML for the diagnosis of SZ are presented in Tables 2 and 3.

Table 2: Summary of studies conducted on the diagnosis of SZ using conventional ML and MRI modalities

Work	Dataset	Miodalites	Number of cases	High Level Prepreprocessing	Preprocessing Toolbox	Feature extraction	Feature reduction/ selection	Classifier	K-fold	Performance criteria(%)
[158]	Clinical	sMRI / rs-fMRI	11 SZ, 11 HC	Segmentation	FreeSurfer / FSL	Amplitude of Low Frequency Fluctuation (ALFF), GM Volume	Linear Kernel Canonical Correlation Analysis (L-kCCA)	NA	–	NA
[159]	Clinical	rs-fMRI	82 SZ, 82 HC	Group Independent Component Analysis (GICA)	SPM / GIFT	Functional Connectivity (FC) Values	T-Test	Affinity Propagation Clustering	–	NA
[160]	Clinical	rs-fMRI	28 SZ, 28 HC	GICA	SPM / REST	Nodes of Functional Connectivity Network (FCN)	PCA	SVM	–	Acc=92.86 Sen=96.43 Spec=92.86
[161]	Clinical	rs-fMRI	48 Adolescent-onset schizophrenia (AOS), 31 HC	–	DPARSF / REST	Mean Regional Homogeneity (ReHo) Values	NA	SVM	–	Acc=90.14 Sen=88.24 Spec=91.89
[162]	Clinical	sMRI	163 SZ, 163 HC	–	FreeSurfer	Average Cortical Thickness and Surface Area	Two-Sample T-Test	SVM	10	Acc=85 Sen=83 Spec=87
[163]	Clinical	rs-fMRI	14 SZ, 14 HC	–	SPM	6 Rigid Body Motion Correction Parameters, BPRS (Brief Psychiatric Rating Scale) and MoCA (The Montreal Cognitive) Scores	NA	NA	–	NA
[164]	Clinical	rs-fMRI	14 SZ, 15 HC	–	CONN / sLORETA / SPM	FC Scores	Paired T-Test / Spearman's Rank Correlation Coefficient	NA	–	NA
[112]	CCNMD	T-fMRI / sMRI	21 SZ, 54 HC	–	SPM	Global and Local Parameters of Functional Connectivity Mean Value of Time Series	Relief Algorithm	SVM	10	Acc=92.1 Sen=92 Spec=92.1 Pre=94
[165]	Clinical	sMRI	41 SZ, 42 NCs	Segmentation, Generalized Linear Model (GLM)	SPM	Between-Group Differences in Gray Matter Volume (GMV), and White Matter Volume (WMV)	Recursive Feature Elimination (RFE)	SVM	–	Acc=88.4 Sen=91.9 Spec=84.4
[114]	Clinical	T-fMRI	155 SZ, 96 HC / 81 SZ, 54 HC	–	DPABI	Multivariate Connectome Features (Mean)	Chi-Squared Test	SVM	5	Acc=71.6
[94]	COBRE	rs-fMRI	70 SZ,70 HC	–	DPABI	Graph Features	Feature Selection via Concave Minimization (FSV)	SVM	10	Acc=95 Sen=96.75 Spec=93.57
[166]	FBIRN Multisite	T-fMRI	84 SZ, 59 HC	GLM, Independent Component Analysis (ICA)	SPM	Singular Value Transform (SVD) Features	Hybrid Multivariate Forward Feature Selection	SVM	–	Acc=94 Sen=96 Spec=92

[167]	Clinical	rs-fMRI	24 SZ, 21 HC	–	SPM	Non-Negative Elastic-Net based Method (N2EN), Discriminant Brain Connectivity Features	Kernel Discriminant Analysis (KDA)	NN	–	Acc=95.56 Sen=100 Spec=90.48
[168]	Clinical	rs-fMRI	52 Chronic SZ, 30 First Episode SZ, 88 HC	Probabilistic Independent Component Analysis (PICA)	FSL	Multivariate Graph Theoretic Measures	Sequential Forward Selection (SFS)	SVM	5	Acc=80 Sen=77 Spec=68
[169]	Clinical	rs-fMRI sMRI	46 SZ, 45 HC	–	SPM Elekta Maxfilter GIFT FSL	Spatial Group Ind- ependent Component Analysis (Sg-ICA) (Static FNC and Dynamic FNC)	Least Absolute Shrinkage and Selection Operator (LASSO) T-test PCA	Ensemble- Learning	–	Acc=87.91
[170]	FBIRN	T-fMRI	55 SZ, 55 HC	–	SPM	Mean	Three-stage Evolutionary Algorithm (GLM, T-Test, NSGA-II) PCA	Linear SVM	–	Acc=99.5
[171]	COBRE	sMRI	30 SZ, 50 HC	Segmentation	NA	Geometrical and Laws Texture Features	NA	NA	–	Dice Similarity=96
[172]	COBRE	rs-fMRI	70 SZ, 74 HC	Fast Fourier Transform (FFT), ICA	ANSI FSL	Different Graph Theoretical Features	NA	SVM	10	Acc=65
[173]	Clinical	sMRI rs-fMRI	NA	–	NA	Multimodal Features	Boruta Algorithm	SVM	–	Acc=94.12 Sen=100 Spec=89.47
[174]	COBRE	rs-fMRI sMRI	78 SZ, 90 HC	–	SPM	Latent Features (Dynamic Functional Network Connectivity)	Elastic Net Regularization (ENR)	Logistic Regression (LR)	10	Acc=71
[175]	Kaggle fMRI Challenge	sMRI T-fMRI	86 Subjects	Spatial ICA (SICA)	SPM GIFT	FNC Features	Attribute Selection with PCA	Naïve Bayes	–	Acc=83.7
[176]	Clinical	rs-fMRI	26 SZ, 26 HC	Group ICA (GICA)	GIFT	Multi Features (Nodes Content Feature, Local Clustering Coefficient)	NA	Multi Kernel SVM	–	Acc=93.1 Sen=100 Spec=84.61
[177]	Multi-Site	rs-fMRI	446 SZ, 451 HC	–	SPM	FC Features	Multi-task Algorithm	LR	10	Acc=86
[178]	Multi-Site	rs-fMRI T-fMRI	80 SZ	Segmentation	SPM	Different Features	NA	Backus- Gilbert	10	Acc=58.6
[179]	Clinical	rs-fMRI	25 SZ, 25 HC	Linear Regression	SPM	Averaging Sliding Time Windows (Dynamic FC Samples)	PCA	K-Means Clustering	–	NA
[180]	COBRE	rs-fMRI	60 SZ, 60 HC	Regression	SPM	Coefficient Maps	Two-sample T-Test	Group-Wise Sparse Representation	–	NA
[181]	Clinical	rs-fMRI	17 SZ, 17 HC	–	SPM REST	Effective Patch- based Feature Extraction Method via Random Forest (Mean Values of All Voxels)	Tree-Guided Group Lasso	SVM	8	Acc=91.1 Sen=94.1 Spec=88.2

Ref	Dataset	Modality	Subjects	Analysis	Software	Features	Method	Classifier	CV	Results
[182]	Clinical	sMRI	13 SZ, 22 HC	–	SPM	Mean Intensities	NA	NA	–	Sen=77 Spec=68
[183]	Clinical	T-fMRI	16 SZ, 22 HC	–	SPM / CMTF	Spatial Activity Maps / Event Related Potentials	Two-Sample T-Test	NA	–	NA
[184]	COBRE NMorphCH NUSDAST	sMRI	276 SZ, 330 HC	–	SPM	Local Grey Matter Volume	LASSO	Enet-TV	5	Acc=68 Sen=68 Spec=68 AUC=74
[185]	Clinical	rs-fMRI	151 SZ, 163 HC	ICA	NA	(dFNC) Between RSN (Resting State Networks) Time Courses, 3D Polarity-coded Volumes	NA	NA	–	NA
[80]	Clinical	sMRI DTI rs-fMRI	40 SZ, 29 HC	sMRI (Segmentation)	FreeSurfer FSL REST SPM	Different Features	Sparse Coding	Multi-kernel SVM	10	Acc=84.29 AUC=81.64 Sen=92.5 Spec=73.33
[186]	MCIC	T-fMRI	81 SZ, 103 HC	–	SPM	Sparsity Parameters	Sparse Multi-Set CCA (sMCCA)	NA	5	NA
[187]	Clinical	sMRI	17 SZ, 17 HC	Segmentation	SPM	Neuroanatomical, Schizotypal and Neurocognitive Variables	RFE	SVM	–	Acc=94 Sen=100 Spec=82.5
[188]	Clinical	T-fMRI	121 SZ, 150 HC	ICA	SPM	Spatial Features	PCA / Two-Sample T-Test	NA	–	NA
[189]	CAMH NUSDAST INNN	sMRI	179 SZ, 220 HC, 50 First Episode Psychosis (FEP)	–	NA	Voxel based Morphometry (VBM)(GM), Regional Analysis of Volumes in Normalized Space (RAVENS) (GM), Cortical Thickness	PCA	SVM	10	Acc=73.5
[120]	NUSDAST	sMRI	104 SZ, 63 NC	Segmentation, CIVET Pipeline	NA	Mean Cortical Thickness Values	Agglomerative Hierarchical Clustering	RF	5	Acc=75 AUC=81
[115]	Clinical	rs-fMRI	48 SZ, 31 HC	–	SPM	FC Values, Mean Framewise Displacement (FD)	T-Test / Chi-squared Test	SVM	–	Acc=92.4 Sen=89.6 Spec=96.8
[190]	Clinical	sMRI DTI	47 SZ, 23 HC	Segmentation	FreeSurfer	Volume and/or Mean Diffusion Measures (FA and Trace)	Minimum Redundancy and Maximum Relevance (mRMR)	SVM	5	Sen=89.5 Spec=94.5
[91]	FBIRN (Multisite Data)	T-fMRI	Data 1: 34 SZ, 34 HC / Data 2: 25 SZ, 25 HC	GLM, ICA	SPM / GIFT	Generalised Discriminant Analysis (GDA) (Non-Linear Features)	Novel Fuzzy Rough Set	SVM	–	Acc=98 Sen=100 Spec=96
[81]	Clinical	rs-fMRI	41 SZ, 38 HC	–	SPM	Different Features	T-Test	SVM	10	Acc=84.7 Sen=91.9 Spec=74.5
[191]	Clinical	rs-fMRI	187 SZ, 173 HC	Linear Regression, Global Signal Regression (GSR)	FSL	Brain-wide Seed-Based Voxel-Wise Analysis (Seed-to-Voxel FCs)	SelectFdr	Gradient Boosting Decision Tree (GBDT)	5	Acc=72.28 AUC=72.77

Ref	Dataset	Modality	Subjects	Preprocessing	Tool	Features	Feature Selection	Classifier	No.	Results
[192]	Clinical	rs-fMRI	48 SZ, 31 HC	–	SPM / Toolkit	Coherence-ReHo Values	Chi-Square Test	SVM	–	Acc=89.87 Sen=91.67 Spec=87.1
[193]	Clinical	sMRI	52 SZ, 66 HC	Segmentation, Gray-white Mater Boundary Tessellation	FreeSurfer / FSL	Cortical and Geometric Features	LASSO	SVM	–	Acc=88 Sen=94 Spec=82
[194]	Clinical	DTI	65 SZ, 60 HC	Segmentation	VISTA-SOFT	Different Features from WM	RFE	RF	10	Acc=76 Sen=76.9 Spec=75
[113]	Clinical	rs-fMRI	51 SZ, 51 HC / 34 SZ, 27 HC	FD	SPM	Spatial–Temporal Reconstruction Based on the ICA (Spatial Components)	Two-Sample T-Test / PCA / Fisher Linear Discriminant	Majority Voting	–	Acc=73 Sen=56.9 Spec=88.2
[195]	Clinical	sMRI / DTI	62 SZ, 33 HC	–	FreeSurfer / FMRIB	Cortical Gray Matter Volume, Cortical Thickness, Mean Diffusivity, Fractional Anisotropy	Minimum Redundancy and Maximum Relevance (mRMR) / RFE	Multi-Kernel SVM (MFMK-SVM)	6	Acc=91.28 Sen=90.85 Spec=92.17 AUC=94.85
[196]	NAMIC	sMRI	20 Subjects	Segmentation	NA	Texture Features	Multi-objective BPSO	Fuzzy SVM (FSVM)	–	Acc=90 Sen=92.86 Spec=87.5
[95]	COBRE	rs-fMRI	71 SZ, 74 HC	–	DPABI	Graph Theoretical Approach (Local Graph Measures)	Sparse Group Lasso	SVM	–	Acc=93.1 Sen=92.96 Spec=93.24
[197]	Clinical	sMRI	23 SZ, 23 Schizo-Obsessive	–	SPM / VBM	Voxel-Based Morphometry (Gray Matter Differences, VOIs)	Ant Colony (ACO)	SVM	6	Acc=78.26 Sen=79 Spec=78
[198]	COBRE	sMRI	34 Paranoid Schizophrenia, 34 NC	Segmentation	SPM	Gray Matter and White Matter Features	RFE / Two-Sample T-Tests	SVM	–	Acc=85.27 Sen=85.87 Spec=85.08
[199]	FBIRN	T-fMRI	55 SZ, 55 HC	–	SPM	Voxel Values	GLM / T-Test / NSGA-II	SVM	–	Acc=95.45
[200]	FBIRN	T-fMRI	Dataset1: 34 SZ, 34 HC / Dataset2: 25 SZ, 25 HC	GLM, Group Spatial ICA (GSICA)	SPM / GIFT	Novel Fuzzy Kernel Principal Component Analysis (FKPCA) (Voxel Values)	Hybrid Forward Feature Selection (Filter-Cum-Wrapper)	SVM	–	Acc=96
[201]	Clinical	sMRI	82 HC, 143 Chronic SZ, 32 FEP Patients	–	FreeSurfer	Structure's Brain Volumes	NA	Maximum Uncertainty Linear Discriminant Analysis (MLDA)	–	Acc=73 Sen=77.6 Spec=68.3
[202]	COBRE / NMorphCH	rs-fMRI	56 SZ, 74 HC / 43, SZ, 39 NC	Segmentation	SPM / REST	FC Strength Between Different Brain Regions	Two Sample T-Test	SVM	20	Acc=80.49 Sen=83.72 Spec=76.92
[203]	MCIC / Genes Dataset	T-fMRI	79, SZ, 103 HC / 75 Genes	–	SPM	Genetic, Imaging and Epigenetics Features (SNPs, Voxels, Methyla-Tions)	KMDHOI	SVM	2	Acc=89.68

Ref	Dataset	Modality	Subjects	Preprocessing	Tool	Features	Feature Selection	Classifier	Folds	Results
[204]	PHAMOUS; International Dataset From 9 Centers; International Dataset with Imaging	rs-fMRI	2035 SZ	–	SPM; CAT12	Demographic and Clinical Features	PCA	Fuzzy C-means Clustering	10	Acc=73
[205]	COBRE	sMRI	57 SZ, 69 HC	Segmentation	FreeSurfer	Structural Features (Hippocampal and Amygdaloid Features)	Sequential Backward Elimination (SBE) Algorithm	SVM	–	Acc=81.75 Sen=84.21 Spec=81.16 AUC=82.41
[206]	Clinical	sMRI	179 SZ, 77 HC	–	FreeSurfer	Regional Cortical Thickness Values	Analysis of Variance (ANOVA)	K-means Clustering	–	–
[207]	MRN; COBRE	sMRI	71 SZ, 74 HC	Segmentation, Markov Random Field (MRF)	VBM	Grey Matter Volume Patterns	PCA	SVM	10	Acc=81.2 Sen=82.6 Spec=79.5
[208]	SchizConnect; OpenfMRI	T-fMRI	191 SZ, 191 HC	–	NIAK	Feature Weights (Functional Brain Connectomes)	NA	SVM	10	Acc=84
[209]	COBRE	rs-fMRI; sMRI	56 SZ, 56 HC	Segmentation	CONN	FCM	Mann–Whitney U test	SVM	8	Acc=69 Sen=68 Spec=72
[210]	Clinical	rs-fMRI; sMRI	42 SZ, 34 Unaffected (First-Degree Relatives), 40 HC	–	SPM; AFNI; FSL	ICA Guided by Group Information (GIG-ICA) (Informative FNs)	Forward Component Selection Algorithm	SVM	10	Acc=83.9 Sen=87.5 Spec=80
[211]	COBRE	rs-fMRI; sMRI	72 SZ, 72 HC	sMRI (Segmentation)	FreeSurfer	Different Features	Hybrid Weighted Feature Concatenation (WC) Method	Extreme Learning Machine (ELM)	10	Acc=92.29 Sen=100 Spec=98.6
[212]	Clinical	rs-fMRI; MRI	76 FE Schizophrenia (FES) Drug Naïve, 74 Ultrahigh Risk, 71 HC	Computation of FD, Linear Detrending	DPABI	Parameter of Functional Asymmetry (PAS) Values	ANOVA	SVM	5	Acc=74.83 Sen=68.42 Spec=81.69
[213]	COBRE	rs-fMRI	60 SZ, 71 HC	–	SPM; REST	Consensus Functional Connections with High Discriminative Power	T-Test	LDA	10	Acc=76.34 Sen=70 Spec=81.69
[214]	–	rs-fMRI	28 SZ, 40 HC, 28 Family-Based Controls	–	DPARSF; T-Test	Short-Range Positive FC Strength (FCS) Long-Range Positive (FCS) Values, Mean z Values	Analyses of Covariance (ANCOVA)	SVM	–	Acc=94.6 Sen=92.86 Spec=96.4
[215]	Multi Datasets	rs-fMRI	295 SZ, 452 HC	–	SPM	Mean Time Series, Graph-Based Metrics	NA	SVM	5	Acc=81
[216]	Clinical	sMRI	38 SZ, 38 HC	–	FreeSurfer	Cortical Thickness (Edge and Node Features)	Minimum Redundancy and Maximum Relevance (mRMR); RFE	SVM	6	Acc=88.72 AUC=95.21 Sen=87.19 Spec=94.27
[217]	COBRE	sMRI	72 SZ, 75 HC	–	NA	Pixels from Segmented Ventricle Regions	NA	NA	NA	R = 0.99 Rand Index=0.98

[88]	Clinical	sMRI	100 SZ, 100 HC	–	SPM	GLCM Features	NA	Extreme Gradient Boosting (XGBoost)	NA	Acc=72 AUC=75.8
[218]	Clinical	sMRI	141 SZ, 71 HC	Segmentation	SPM	Key Neuroanatomical Features	ROI Selection Algorithm	SVM	NA	Acc=89.4 Sen=96.6 Spec=74.1
[219]	Clinical	sMRI	138 SZ, 151 HC	–	FreeSurfer / FSL	Different Features	Probabilistic PCA (PPCA)	Ensemble of Trees Algorithm	3	Balanced Acc=64.2
[220]	Combination of Five Datasets	sMRI / rs-fMRI	295 SZ, 452 HC	sMRI (Segmentation)	SPM / DPARSF	Gray Matter and White Matter Volume, Structural Covariance Matrix, ALFF, ReHo, FCM	NA	SVM	10	Acc=90.83 Sen=84.69 Spec=96.97
[221]	Clinical	sMRI / DTI	57 SZ	–	Different Toolboxes	Radiomic Features	LASSO	Support Vector Regression (SVR)	NA	–
[89]	NAMIC / COBRE	rs-fMRI	8 SZ, 10 HC / 69 SZ, 74 HC	ICA	SPM	Orthogonal Ripplet Transform Type II	Two-sample T-test / Orthogonal Locality Preserving Projection	SVM	5	Probability of Correct Classification (Pcc)=100
[222]	B-SNIP	sMRI	176 BP Probands / 134 SZ Disorder Probands / 240 SZ Probands / 362 HC	Segmentation	SPM	Voxels of Brain Images	ANOVA	SVM	NA	Acc=89
[223]	Clinical	DTI	41 Bipolar Disorder, 39 SZ, 23 HC	–	TBSS	Average Fractional Anisotropy Values	GA	Artificial Neural Network	4	Acc=81.25 AUC=83
[224]	Schizconnect / NAMIC	sMRI / rs-MRI	81 SZ, 82 HC	sMRI (Segmentation)	NA	Radiomic Features	Feature selection Based on BPSO	Fuzzy Support Vector Machine (FSVM)	3	Acc=90.09 Sen=94.42 Spec=95.48
[225]	NBH / COBRE / Huaxi / Nottingham / Taiwan / Xiangya	rs-fMRI	21 SZ, 24 HC / 53 SZ, 67 HC / 178 SZ, 180 HC / 32 SZ, 36 HC / 69 SZ, 62 HC / 83 SZ, 60 HC	–	SPM / DPARSF	FCN (Topological Features)	Kernel Discriminant Analysis (KDA)	KNN	10	Acc=94.22 Sen=94.69 Spec=94.93 F1-Score=94.36

Table 3: Summary of studies conducted on the diagnosis of SZ using DL and MRI modalities

Work	Dataset	Modalities	Number of cases	High Level Prepreprocessing	Preprocessing Toolbox	DNN	DNN toolbox	Classifier	K- fold	Performance criteria(%)
[226]	NUSDAST / IMH	sMRI	141 SZ, 134 HC / 148 SZ, 76 HC	Segmentation	NA	Inception-ResNet	NA	SVM	5	Acc=70.98 Spec=63.16 Sen=75
[227]	FBIRN phase-II fMRI	T-fMRI	46 SZ, 49 HC	tCompCor Denoising	FSL	LSTM	NA	NA	10	Test Performance=66.4
[228]	Clinical	rs-fMRI	39 SZ, 31 HC	–	SPM	AE	NA	ANN	10	Acc=79.3 Sen=87.4 Spec=82.2
[229]	Clinical	rs-fMRI	42 SZ, 40 HC	ICA	SPM	2D-CNN	NA	Softmax	5	Acc=90.79 Sen=92.12 Spec=90.67

29

[230]	Clinical	rs-fMRI	558 SZ, 542 HC	ICA, PCA	SPM / GIFT	DNN+LPR	TensorFlow	Softmax	10	Acc=84.75 Sen=86.68 Spec=82.79 F1-Score=85
[231]	COBRE	rs-fMRI	72 SZ, 72 HC	ICA	FSL	VGGNet	TensorFlow	Softmax	10	Acc=98.09 Sen=97.49 Spec=98.62
[232]	Clinical	sMRI	143 SZ, 83 HC, 32 First-Episode Psychosis	Multiple Linear Regression (MLR)	NA	DBN	Theano	Softmax	3	Acc=73.6 Sen=76.37 Spec=70.74
[233]	MCIC (SNP and fMRI Dataset)	T-fMRI	80 SZ, 103 HC	Multiple Regression Mission Measurements (MRMM)	SPM	Deep Canonically Correlated Sparse AE (DCCSAE)	TensorFlow	SVM	–	Acc =80.53
[234]	Clinical	T-fMRI	103 SZ, 41 HC	–	SPM	3D-CAE	Keras	Softmax	10	Acc=84.43 Sen=88.42 Spec=80.06
[235]	Clinical	rs-fMRI T-fMRI sMRI	96 SZ, 115 HC	–	SPM	1D-CNN	NA	Two Step Ridge Classifier	10	Acc=87
[236]	Multi-site (7 sites)	rs-fMRI	558 SZ, 542 HC	ICA	SPM / GIFT	CNN-GRU	Keras	Softmax	10	Acc=83.2 AUC=90.6 Sen=83.1 Spec=83.5 F1-Score=83.3
[237]	SchizConnect (BrainGluSchi, COBRE, MCICShare, NMorphCH, NUSDAST)	sMRI	473 SZ, 453 HC	Segmentation	MRIcron	3D-CNN	NA	Softmax	10	Acc=70 AUC=72 Sen=81.6 Spec=47.1
[238]	COBRE	rs-fMRI Pheno-typic Informa-tion	72 SZ, 74 HC	Segmentation	NA	DBN	NA	Softmax	3	Acc=90 AUC=89.9 Sen=87.5 Spec=92.86 Pre=93.33
[239]	Clinical	sMRI	198 SZ, 191 HC	Segmentation, PCA	SPM / GIFT	RBM	NA	NA	–	NA
[240]	HDLSS	sMRI rs-fMRI	69 SZ, 75 HC	–	NA	DCNN	Keras TensorFlow	Sigmoid	–	Acc=82.35 AUC=81.28
[241]	Multi-site (COBRE, FBIRN)	sMRI rs-fMRI	144 SZ, 154 HC 98 SZ, 91 HC	sMRI: ICA rs-fMRI: GICA	SPM INRIAlign GIFT	DCNN	NA	Softmax	–	Different Results
[242]	Multi-site	rs-fMRI	357 SZ, 377 HC	–	SPM	Deep Discriminant AE with Sparsity Constraint (DANS)	NA	SVM	10	Acc=85
[243]	COBRE	sMRI rs-fMRI	60 SZ, 71 HC	Segmentation	SPM	CapsNet	NA	Softmax	10	Acc=82.42 Sen=88.57 Spec=75
[244]	COBRE UCLA WUSTL	rs-fMRI	102 SZ, 120 HC	–	SPM	CapsNet	TensorFlow	Softmax	10	Acc=82.83 AUC=91.4

Ref	Dataset	Modality	Subjects	Method	Toolbox	DL Method	Framework	Classifier	K-fold	Results
[245]	Clinical	sMRI, rs-fMRI	86 Labeled and 119748 Unlabeled Data	GICA	SPM	Deep Canonically Correlated AE (DCCAE)	NA	SVM	–	AUC=95
[246]	MCIC	rs-fMRI, SNP	81 SZ, 103 HC	Data Augmentation (DA), Segmentation using K-means	SPM	Deep Principal Correlated AE (DPCAE)	TensorFlow	Sigmoid	5	Acc=93.8
[247]	Multi Sites	sMRI	662 SZ, 613 HC	NA	FreeSurfer	DNN Based Layer-wise Relevance Propagation (LRP)	NA	Softmax	10	Acc=76.82 Sen=76.85 Spec=76.17 AUC=77.27
[248]	Clinical	rs-fMRI, sMRI	69 SZ, 75 HC	ICA	NA	DCNN	Keras	Sigmoid	–	Acc=94.44
[249]	COBRE	fMRI	72 SZ, 74 HC	Segmentation	SPM	SAE	NA	SVM	10	Acc=92 F1-Score=92.27
[250]	COBRE, UCLA	rs-fMRI	72 SZ, 75 HC; 138 SZ, 58 HC	Segmentation, PCA	DPABI	Weighted Deep Forest (gcForest)	NA	Softmax	10	Acc=61 Sen=63 Spec=54
[251]	COBRE	rs-fMRI	50 SZ, 50 HC	GICA	SPM, ArtRepair, GIFT	SAE	MATLAB	Softmax	5	Sen=85.3 Spec=87.5
[130]	NUSDAST	sMRI	35 SZ, 40 HC	Segmentation	FreeSurfer	AE	Keras, TensorFlow	SVM	10	Acc=86.25
[252]	OpenfMRI	rs-fMRI	48 SZ, 46 BPs, 117 NCs	Segmentation	NA	GAN	TensorFlow	Different Methods	10	BACC=71.3 MCC=43.8 F1-Score=58.1
[253]	ADHD-200, Clinical	rs-fMRI, sMRI	587 sMRI; 28 SZ, 28 HC	–, Segmentation	SPM, NA	3D-CNN	TensorFlow	Softmax	5	Acc=81.8 Sen=77.4 Spec=86.2
[254]	COBRE	rs-fMRI	69 SZ, 72 HC	–	CONN	DNN	DCNN	Softmax	–	Acc=77.8
[255]	Multi-sites Datasets	rs-fMRI	558 SZ, 542 HC; 269 Major Depressive Disorder, 286 HC	Group-ICA	SPM, GIFT	GAN	Theano	Softmax	10	Acc=82.1 Sen=78.1 Spec=86.2 AUC=82.3
[256]	Kyoto University dataset, COBRE	sMRI	82 SZ, 90 HC; 71 SZ, 71HC	Segmentation	SPM	3D-CAE	NA	LR	5	P-Value=96.8
[257]	Clinical Datasets	T-fMRI	46 SZ, 2BP, 55 HC; 54 SZ, 49 BP, 122 HC	Segmentation	NA	V-Net	NA	SVM	5	AUC=86.3
[258]	Clinical	sMRI	171 SZ, 142 HC	Segmentation	SPM	GAN	NA	SVM	10	Acc=87.1

4. Discussion

This paper provides a comprehensive overview of SZ diagnosis methods using MRI modalities and AI techniques. Since 2016 DL methods have paved the way for the diagnosis of SZ using MRI modalities; thus, only studies performed after that have been included in this review. The reason for this is to make a valid comparison between studies that used conventional ML methods over DL

in the diagnosis of SZ. All studies on the diagnosis of SZ have been reviewed using sMRI and fMRI neuroimaging modalities along with DL and conventional ML methods in Tables 2 and 3. Table 2 shows the important information for schizophrenia diagnosis using conventional ML, including dataset types, modalities, preprocessing techniques, preprocessing toolboxes, feature extraction, feature selection / reduction, classification, K-Fold, and finally evaluation parameters. Similarly, Table 3 focuses on DL methods, including DL architecture, DL toolboxes, and classification methods. Figure 11 shows the number of papers published on conventional ML and DL for automated SZ detection using MRI modalities.
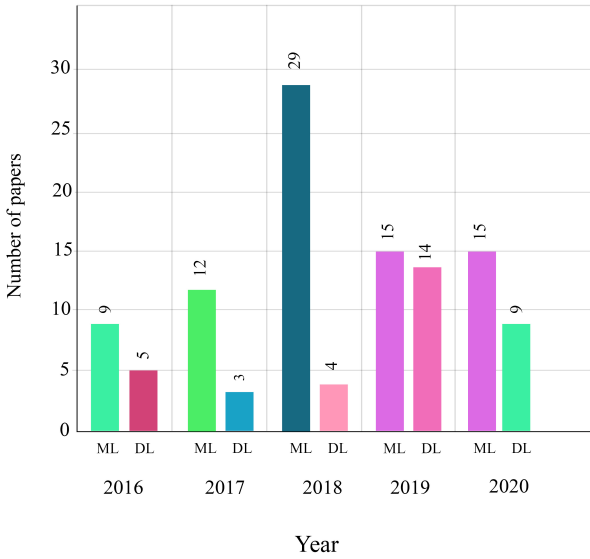
Figure 11: Number of papers published on conventional ML and DL for automated SZ detection using MRI modalities.

It can be noted from Figure 11 that, conventional ML has been used more than DL for the automated SZ detection. This may be because there are limited numbers of public MRI datasets available. Secondly, conventional ML methods do not require powerful hardware resources, and by selecting less complex features, high performance can be achieved.

It can be noted from Table 1 that, several freely available datasets are available for automated diagnosis of SZ. The various methods which have been proposed using these free datasets are shown in Tables 2 and 3. The number of datasets used to develop DL and ML models proposed each year is displayed in Figure 12. It can be noted from this figure that, the COBRE dataset is more efficient and popular than other datasets for the studies on automated detection of SZ. As illustrated in Figure 12, the COBRE dataset is of more significance than the rest because the size of normal and schizophrenia classes are equal in this dataset.
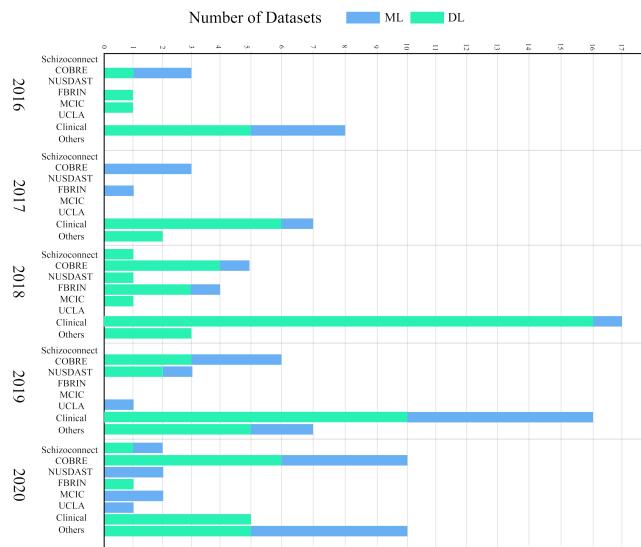
Figure 12: Number of studies published in the last four years on automated SZ detection using different MRI-based datasets.

Figure 13 shows the types of sMRI and fMRI neuroimaging modalities used for the diagnosis of SZ in Tables 2 and 3. It can be seen that rs-fMRI neuroimaging modality has been widely used. Also, it can be noted from the figure that, in recent years more studies have been conducted on automated SZ using sMRI and rs-fMRI neuroimaging modalities.

Preprocessing of sMRI and fMRI modalities is an important step in the
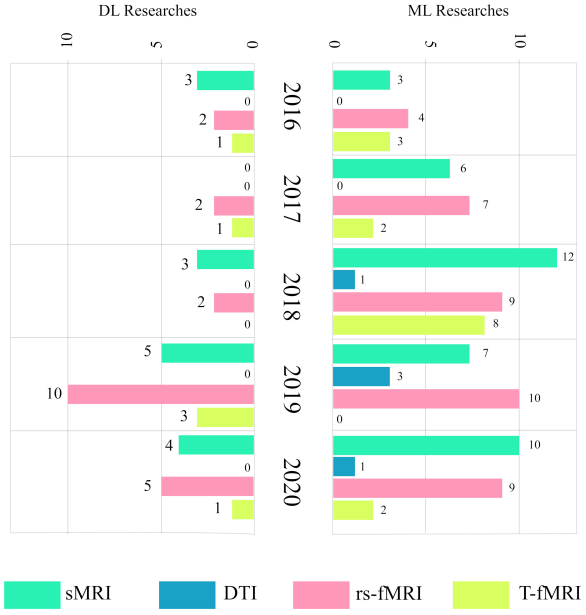
Figure 13: Number of studies published in the last four years on automated SZ detection using different MRI modalities and AI methods.

automated detection of SZ. The preprocessing techniques are divided into two categories of low-level and high-level methods, which were described in details in the previous sections. Low-level preprocessing using sMRI or fMRI modalities have specific and standard steps. Hence, FSL [65], BET [259, 260], FreeSurfer [67] and SPM [68] tools have been introduced for low-level preprocessing. The number of preprocessing tools used for the automated diagnosis of SZ is shown in Figure 14. It can be noted from this figure that, SPM toolbox has been widely used by the researchers.

The number of MRI-based studies published after 2016 for automated detection of SZ using different AI techniques is presented in Figure 15. It can be noted from Figure Figure 15(a) that, Softmax method is widely used for classification. The SVM classifier is widely used for classification purposes in ML method (Figure Figure 15(b)).
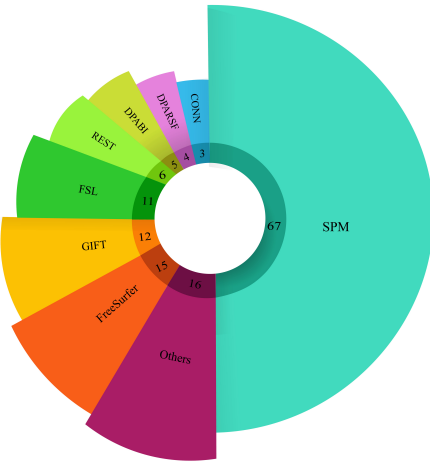
Figure 14: Number of preprocessing tools used for the automated diagnosis of SZ.

5. Challenges

Challenges in the design of automated detection of SZ using MRI modalities and AI techniques are described in this section. Data constraints, algorithmic and hardware problems are the most important challenges in this field, which are discussed below. There are few freely available sfMRI and fMRI datasets (Table 1). This has prevented researchers from proposing novel DL models. Hence, more ML models have been proposed which work with a limited number of data samples. Also, the lack of access to all spatially high-resolution sMRI and DTI and spatially-temporally high resolution fMRI datasets are other challenges in this field that avoid researchers to evaluate the effectiveness of simultaneous usage of these MRI modalities to diagnose SZ. The other challenge is to accurately diagnose different types of SZ using sMRI and fMRI modalities. The Schizconnect dataset offers different classes of SZ, but the number of subjects and the variety of chronic disorders are so limited that it is difficult to use them for practical applications. Other available datasets have only SZ and normal classes. Therefore, providing datasets with a large number of subjects and different types of SZ disorders will help researchers to develop a clinically useful
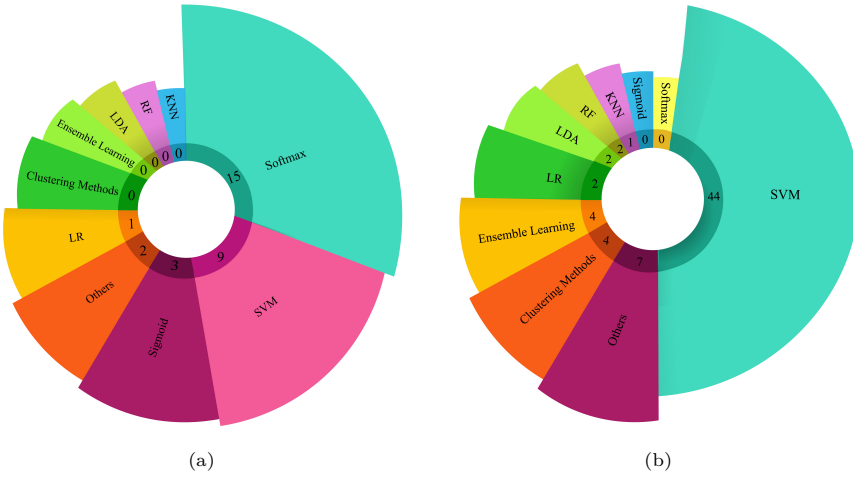
Figure 15: Number of MRI-based studies published after 2016 for automated detection of SZ using different AI techniques: (a) DL and (b) ML.

system.

In practical applications, we also need to diagnose mental disorders with symptoms close to each other. For example, it is sometimes challenging to diagnose SZ from Bipolar disorder [261] and ADHD [262] based on symptoms. Creating a large dataset of patients with these mental disorders, although difficult, can be of great help to physicians in diagnosing SZ accurately.

Early detection and predicting the SZ are very important and challenging tasks. However, due to the difficulty in collecting such datasets (due to the need for longitudinal studies and follow-up of individuals over time), little research has been done in this area and deserves more attention.

Another challenge is related to the use of AI techniques (DL and conventional ML). Implementing CADS based on conventional ML requires a great deal of knowledge in AI. Extracting the distinguishing features which can lead to effective SZ biomarkers is the most important part of CADS. The development of DL architectures for the diagnosis of SZ has been challenging task due to lack of access to appropriate hardware resources and data availability. Although websites like Google Colab, Amazon, etc. now provide researchers with

high computing processors, implementing these methods and using them in the real world still poses many problems.

6. Conclusion and Future Works

Schizophrenia is a mental disorder that directly affects the brain, causing symptoms such as abnormal speech and reduced ability to understand. In this work, we have summarized various automated systems developed using MRI neuroimaging modalities to detect SZ early and accurately. Our findings show that, compared to other diagnostic methods, sMRI and fMRI neuroimaging modalities provide physicians with important information about brain function which helps to accurately diagnose SZ. In these types of neuroimaging modalities, parts of SZ brain do not have a normal structure or function and are usually recognizable. In addition to the benefits of MRI modalities, analyzing this data to diagnose SZ by a physician is complex. To this end, conventional ML and DL techniques have been combined with MRI modalities to assist the clinicians to make an accurate diagnosis of SZ. In this article, a complete review of the diagnosis of SZ with the help of sMRI and fMRI neuroimaging modalities along with DL methods and conventional ML has been done. In the discussion section of this article, a detailed review is conducted on research conducted in the field of DL compared to conventional ML. As discussed, lots of work has been done in automated diagnosis of SZ using conventional ML and DL techniques. The DL networks require a lot of data for training, and the lack of free and available datasets are the main reason for the main challenge in the automated diagnosis of SZ accurately.

Different models of GANs are one of the newest areas of DL that can be used to address this data shortage problem [136]. In future work, DL networks such as deep convolutional GAN (DCGAN) [263, 264] will largely address these problems of MRI data shortages to expand DL applications in diagnosing SZ from healthy subjects. Also, as mentioned earlier, the free Schizconnect dataset contains sMRI and fMRI neuroimaging modalities of various schizophrenic dis-

orders. The generation of artificial data from different classes of SZ with the help of GAN architectures can be considered as the future work in designing a CAD system for effective diagnosis of this disease. So far, we have reviewed potential future works on the generation of artificial data and increasing the efficiency of CADS for the diagnosis of SZ. Another challenge is the lack of free access to sMRI or fMRI neuroimaging modalities for a particular class of SZ. Zero-shot learning is a new class of AI techniques which can solve the problem of not having access to the data of a class of SZ and is considered as another future work [265, 266].

Different types of SZ are growing in less developed countries. Lack of access to specialist physicians to analyze sMRI and fMRI data is always a challenge. In future, the practical implementation of CADS based on DL and cloud computing can greatly provide valuable services to people with these brain disorders. The sMRI or fMRI scan can be sent to the cloud where the accurate DL model can be placed. The result of the model will be sent to the hospital server. After confirmation with the specialist clinician, the diagnosis will results can be sent to the patient.

Acknowledgement

References

[1] C. Ross, Schizophrenia: Innovations in diagnosis and treatment, Routledge, 2014.

[2] N. C. Andreasen, W. T. Carpenter Jr, Diagnosis and classification of schizophrenia, Schizophrenia bulletin 19 (2) (1993) 199–214. `doi:10.1093/schbul/19.2.199`.

[3] S. J. Bartels, R. E. Drake, Depressive symptoms in schizophrenia: comprehensive differential diagnosis, Comprehensive Psychiatry 29 (5) (1988) 467–483. `doi:10.1016/0010-440X(88)90062-4`.

[4] R. Tandon, et al., Antipsychotics in the treatment of schizophrenia: an overview, The Journal of clinical psychiatry 72 (suppl 1) (2011) 4–8. `doi: 10.4088/JCP.10075su1.01`.

[5] M. Kubicki, R. McCarley, C.-F. Westin, H.-J. Park, S. Maier, R. Kikinis, F. A. Jolesz, M. E. Shenton, A review of diffusion tensor imaging studies in schizophrenia, Journal of psychiatric research 41 (1-2) (2007) 15–30. `doi:10.1016/j.jpsychires.2005.05.005`.

[6] C. Tamminga, H. Holcomb, Phenotype of schizophrenia: a review and formulation, Molecular psychiatry 10 (1) (2005) 27–39. `doi:10.1038/sj.mp.4001563`.

[7] https://en.wikipedia.org/wiki/schizophrenia.

[8] A. M. Shepherd, K. R. Laurens, S. L. Matheson, V. J. Carr, M. J. Green, Systematic meta-review and quality assessment of the structural brain alterations in schizophrenia, Neuroscience & Biobehavioral Reviews 36 (4) (2012) 1342–1356. `doi:10.1016/j.neubiorev.2011.12.015`.

[9] D. W. Heinrichs, R. W. Buchanan, Significance and meaning of neurological signs in schizophrenia., The American journal of psychiatry`doi:10.1176/ajp.145.1.11`.

[10] M. P. Boks, S. Russo, R. Knegtering, R. J. van den Bosch, The specificity of neurological signs in schizophrenia: a review, Schizophrenia Research 43 (2-3) (2000) 109–116. `doi:10.1016/S0920-9964(99)00145-0`.

[11] Z. Y. Wee, S. W. L. Yong, Q. H. Chew, C. Guan, T. S. Lee, K. Sim, Actigraphy studies and clinical and biobehavioural correlates in schizophrenia: a systematic review, Journal of Neural Transmission 126 (5) (2019) 531–558. `doi:10.1007/s00702-019-01993-2`.

[12] J. Tomasik, E. Schwarz, P. C. Guest, S. Bahn, Blood test for schizophrenia, European archives of psychiatry and clinical neuroscience 262 (2) (2012) 79–83. `doi:10.1007/s00406-012-0354-3`.

[13] M. E. Shenton, R. Kikinis, F. A. Jolesz, S. D. Pollak, M. LeMay, C. G. Wible, H. Hokama, J. Martin, D. Metcalf, M. Coleman, et al., Abnormalities of the left temporal lobe and thought disorder in schizophrenia: a quantitative magnetic resonance imaging study, New England Journal of Medicine 327 (9) (1992) 604–612. `doi:10.1056/NEJM199208273270905`.

[14] S. G. Siris, Diagnosis of secondary depression in schizophrenia: implications for dsm-iv, Schizophrenia Bulletin 17 (1) (1991) 75–98. `doi: 10.1093/schbul/17.1.75`.

[15] M. Maj, Critique of the dsm–iv operational diagnostic criteria for schizophrenia, The British Journal of Psychiatry 172 (6) (1998) 458–460. `doi:10.1192/bjp.172.6.458`.

[16] P. McGuire, O. D. Howes, J. Stone, P. Fusar-Poli, Functional neuroimaging in schizophrenia: diagnosis and drug discovery, Trends in pharmacological sciences 29 (2) (2008) 91–98. `doi:10.1016/j.tips.2007.11.005`.

[17] C. Aine, H. J. Bockholt, J. R. Bustillo, J. M. Cañive, A. Caprihan, C. Gasparovic, F. M. Hanlon, J. M. Houck, R. E. Jung, J. Lauriello, et al., Multimodal neuroimaging in schizophrenia: description and dissemination, Neuroinformatics 15 (4) (2017) 343–364. `doi:10.1007/ s12021-017-9338-9`.

[18] K. Sim, I. DeWitt, T. Ditman, M. Zalesak, I. Greenhouse, D. Goff, A. P. Weiss, S. Heckers, Hippocampal and parahippocampal volumes in schizophrenia: a structural mri study, Schizophrenia bulletin 32 (2) (2006) 332–340. `doi:10.1093/schbul/sbj030`.

[19] M. E. Shenton, C. C. Dickey, M. Frumin, R. W. McCarley, A review of

mri findings in schizophrenia, Schizophrenia research 49 (1-2) (2001) 1–52. doi:10.1016/S0920-9964(01)00163-3.

[20] J. J. Wisco, G. Kuperberg, D. Manoach, B. T. Quinn, E. Busa, B. Fischl, S. Heckers, A. G. Sorensen, Abnormal cortical folding patterns within broca's area in schizophrenia: evidence from structural mri, Schizophrenia research 94 (1-3) (2007) 317–327. doi:10.1016/j.schres.2007.03.031.

[21] M. Kyriakopoulos, T. Bargiotas, G. J. Barker, S. Frangou, Diffusion tensor imaging in schizophrenia, European Psychiatry 23 (4) (2008) 255–273. doi:10.1016/j.eurpsy.2007.12.004.

[22] M. Kubicki, R. McCarley, C.-F. Westin, H.-J. Park, S. Maier, R. Kikinis, F. A. Jolesz, M. E. Shenton, A review of diffusion tensor imaging studies in schizophrenia, Journal of psychiatric research 41 (1-2) (2007) 15–30. doi:10.1016/j.jpsychires.2005.05.005.

[23] V. A. Diwadkar, P. Pruitt, D. Goradia, E. Murphy, N. Bakshi, M. S. Keshavan, U. Rajan, A. Reid, C. Zajac-Benitez, Fronto-parietal hypo-activation during working memory independent of structural abnormalities: conjoint fmri and smri analyses in adolescent offspring of schizophrenia patients, Neuroimage 58 (1) (2011) 234–241. doi:10.1016/j.neuroimage.2011.06.033.

[24] A. Varshney, C. Prakash, N. Mittal, P. Singh, A multimodel approach for schizophrenia diagnosis using fmri and smri dataset, in: The International Symposium on Intelligent Systems Technologies and Applications, Springer, 2016, pp. 869–877. doi:10.1007/978-3-319-47952-1_69.

[25] S. L. Oh, J. Vicnesh, E. J. Ciaccio, R. Yuvaraj, U. R. Acharya, Deep convolutional neural network model for automated diagnosis of schizophrenia using eeg signals, Applied Sciences 9 (14) (2019) 2870. doi:10.3390/app9142870.

[26] A. Fernández, M.-I. López-Ibor, A. Turrero, J.-M. Santos, M.-D. Morón, R. Hornero, C. Gómez, M. A. Méndez, T. Ortiz, J. J. López-Ibor, Lempel–ziv complexity in schizophrenia: A meg study, Clinical neurophysiology 122 (11) (2011) 2227–2235. `doi:10.1016/j.clinph.2011.04.011`.

[27] M. Dadgostar, S. K. Setarehdan, S. Shahzadi, A. Akin, Classification of schizophrenia using svm via fnirs, Biomedical Engineering: Applications, Basis and Communications 30 (02) (2018) 1850008. `doi:10.4015/ S1016237218500084`.

[28] H. Song, L. Chen, R. Gao, I. I. M. Bogdan, J. Yang, S. Wang, W. Dong, W. Quan, W. Dang, X. Yu, Automatic schizophrenic discrimination on fnirs by using complex brain network analysis and svm, BMC medical informatics and decision making 17 (3) (2017) 1–9. `doi:10.1186/ s12911-017-0559-5`.

[29] H. Yang, J. Liu, J. Sui, G. Pearlson, V. D. Calhoun, A hybrid machine learning method for fusing fmri and genetic data: combining both improves classification of schizophrenia, Frontiers in human neuroscience 4 (2010) 192. `doi:10.3389/fnhum.2010.00192`.

[30] K. Rubia, T. Russell, E. T. Bullmore, W. Soni, M. J. Brammer, A. Simmons, E. Taylor, C. Andrew, V. Giampietro, T. Sharma, An fmri study of reduced left prefrontal activation in schizophrenia during normal inhibitory function, Schizophrenia research 52 (1-2) (2001) 47–55. `doi: 10.1016/S0920-9964(00)00173-0`.

[31] C. Devia, R. Mayol-Troncoso, J. Parrini, G. Orellana, A. Ruiz, P. E. Maldonado, J. I. Egaña, Eeg classification during scene free-viewing for schizophrenia detection, IEEE Transactions on Neural Systems and Rehabilitation Engineering 27 (6) (2019) 1193–1199. `doi:10.1109/TNSRE. 2019.2913799`.

[32] C.-R. Phang, F. Noman, H. Hussain, C.-M. Ting, H. Ombao, A multi-domain connectome convolutional neural network for identifying

schizophrenia from eeg connectivity patterns, IEEE journal of biomedical and health informatics 24 (5) (2019) 1333–1343. `doi:10.1109/JBHI.2019.2941222`.

[33] C.-R. Phang, C.-M. Ting, F. Noman, H. Ombao, Classification of eeg-based brain connectivity networks in schizophrenia using a multi-domain connectome convolutional neural network, arXiv preprint arXiv:1903.08858.

[34] W.-L. Chu, M.-W. Huang, B.-L. Jian, K.-S. Cheng, Analysis of eeg entropy during visual evocation of emotion in schizophrenia, Annals of general psychiatry 16 (1) (2017) 1–9. `doi:10.1186/s12991-017-0157-z`.

[35] Z. Dezhina, S. Ranlund, M. Kyriakopoulos, S. C. Williams, D. Dima, A systematic review of associations between functional mri activity and polygenic risk for schizophrenia and bipolar disorder, Brain imaging and behavior 13 (3) (2019) 862–877. `doi:10.1007/s11682-018-9879-z`.

[36] G. M. Giordano, M. Stanziano, M. Papa, A. Mucci, A. Prinster, A. Soricelli, S. Galderisi, Functional connectivity of the ventral tegmental area and avolition in subjects with schizophrenia: a resting state functional mri study, European Neuropsychopharmacology 28 (5) (2018) 589–602. `doi:10.1016/j.euroneuro.2018.03.013`.

[37] J. I. Friedman, C. Tang, D. Carpenter, M. Buchsbaum, J. Schmeidler, L. Flanagan, S. Golembo, I. Kanellopoulou, J. Ng, P. R. Hof, et al., Diffusion tensor imaging findings in first-episode and chronic schizophrenia patients, American Journal of Psychiatry 165 (8) (2008) 1024–1032. `doi:10.1176/appi.ajp.2008.07101640`.

[38] M. Kyriakopoulos, N. S. Vyas, G. J. Barker, X. A. Chitnis, S. Frangou, A diffusion tensor imaging study of white matter in early-onset schizophrenia, Biological psychiatry 63 (5) (2008) 519–523. `doi:10.1016/j.biopsych.2007.05.021`.

[39] G. D. Pearlson, Functional mri findings in schizophrenia, in: Neuroimaging in Schizophrenia, Springer, 2020, pp. 113–124. `doi:10.1007/978-3-030-35206-6_6`.

[40] J. Gong, J. Wang, X. Luo, G. Chen, H. Huang, R. Huang, L. Huang, Y. Wang, Abnormalities of intrinsic regional brain activity in first-episode and chronic schizophrenia: a meta-analysis of resting-state functional mri, Journal of psychiatry & neuroscience: JPN 45 (1) (2020) 55. `doi:10.1503/jpn.180245`.

[41] B. K. Brent, H. W. Thermenos, M. S. Keshavan, L. J. Seidman, Gray matter alterations in schizophrenia high-risk youth and early-onset schizophrenia: a review of structural mri findings, Child and Adolescent Psychiatric Clinics 22 (4) (2013) 689–714. `doi:10.1016/j.chc.2013.06.003`.

[42] R. W. McCarley, C. G. Wible, M. Frumin, Y. Hirayasu, J. J. Levitt, I. A. Fischer, M. E. Shenton, Mri anatomy of schizophrenia, Biological psychiatry 45 (9) (1999) 1099–1119. `doi:10.1016/S0006-3223(99)00018-9`.

[43] J. E. Anderson, C. G. Wible, R. W. McCarley, M. Jakab, K. Kasai, M. E. Shenton, An mri study of temporal lobe abnormalities and negative symptoms in chronic schizophrenia, Schizophrenia research 58 (2-3) (2002) 123–134. `doi:10.1016/S0920-9964(01)00372-3`.

[44] M. Fjellvang, L. Grøning, U. K. Haukvik, Imaging violence in schizophrenia: a systematic review and critical discussion of the mri literature, Frontiers in psychiatry 9 (2018) 333. `doi:10.3389/fpsyt.2018.00333`.

[45] E. Veronese, U. Castellani, D. Peruzzo, M. Bellani, P. Brambilla, Machine learning approaches: from theory to application in schizophrenia, Computational and mathematical methods in medicine 2013. `doi:10.1155/2013/867924`.

[46] G. Starke, E. De Clercq, S. Borgwardt, B. S. Elger, Computing schizophre-

nia: Ethical challenges for machine learning in psychiatry, Psychological Medicine (2020) 1–7`doi:10.1017/S0033291720001683`.

[47] G. Cho, J. Yim, Y. Choi, J. Ko, S.-H. Lee, Review of machine learning algorithms for diagnosing mental illness, Psychiatry investigation 16 (4) (2019) 262. `doi:10.30773/pi.2018.12.21.2`.

[48] J. M. Górriz, J. Ramírez, A. Ortíz, F. J. Martínez-Murcia, F. Segovia, J. Suckling, M. Leming, Y.-D. Zhang, J. R. Álvarez-Sánchez, G. Bologna, et al., Artificial intelligence within the interplay between natural and artificial computation: Advances in data science, trends and applications, Neurocomputing 410 (2020) 237–270. `doi:10.1016/j.neucom.2020.05.078`.

[49] A. Shoeibi, N. Ghassemi, R. Alizadehsani, M. Rouhani, H. Hosseini-Nejad, A. Khosravi, M. Panahiazar, S. Nahavandi, A comprehensive comparison of handcrafted features and convolutional autoencoders for epileptic seizures detection in eeg signals, Expert Systems with Applications 163 (2021) 113788. `doi:10.1016/j.eswa.2020.113788`.

[50] N. Ghassemi, A. Shoeibi, M. Rouhani, H. Hosseini-Nejad, Epileptic seizures detection in eeg signals using tqwt and ensemble learning, in: 2019 9th International Conference on Computer and Knowledge Engineering (ICCKE), IEEE, 2019, pp. 403–408. `doi:10.1109/ICCKE48569.2019.8964826`.

[51] M. Khodatars, A. Shoeibi, N. Ghassemi, M. Jafari, A. Khadem, D. Sadeghi, P. Moridian, S. Hussain, R. Alizadehsani, A. Zare, et al., Deep learning for neuroimaging-based diagnosis and rehabilitation of autism spectrum disorder: A review, arXiv preprint arXiv:2007.01285.

[52] M. Rahman, O. L. Usman, R. C. Muniyandi, S. Sahran, S. Mohamed, R. A. Razak, et al., A review of machine learning methods of feature selection and classification for autism spectrum disorder, Brain sciences 10 (12) (2020) 949. `doi:10.3390/brainsci10120949`.

[53] Y. Zhang-James, E. C. Helminen, J. Liu, B. Franke, M. Hoogman, S. V. Faraone, E.-A. working group, et al., Machine learning classification of attention-deficit/hyperactivity disorder using structural mri data, bioRxiv (2019) 546671`doi:10.1101/546671`.

[54] C.-Y. Cheng, W.-L. Tseng, C.-F. Chang, C.-H. Chang, S. S.-F. Gau, A deep learning approach for missing data imputation of rating scales assessing attention-deficit hyperactivity disorder, Frontiers in psychiatry 11 (2020) 673. `doi:10.3389/fpsyt.2020.00673`.

[55] H. G. Schnack, M. Nieuwenhuis, N. E. van Haren, L. Abramovic, T. W. Scheewe, R. M. Brouwer, H. E. H. Pol, R. S. Kahn, Can structural mri aid in clinical classification? a machine learning study in two independent samples of patients with schizophrenia, bipolar disorder and healthy subjects, Neuroimage 84 (2014) 299–306. `doi:10.1016/j.neuroimage.2013.08.053`.

[56] D. Chyzhyk, M. Grana, D. Öngür, A. K. Shinn, Discrimination of schizophrenia auditory hallucinators by machine learning of resting-state functional mri, International journal of neural systems 25 (03) (2015) 1550007. `doi:10.1142/S0129065715500070`.

[57] S. Iwabuchi, P. F. Liddle, L. Palaniyappan, Clinical utility of machine-learning approaches in schizophrenia: improving diagnostic confidence for translational neuroimaging, Frontiers in psychiatry 4 (2013) 95. `doi:10.3389/fpsyt.2013.00095`.

[58] http://www.schizconnect.org.

[59] L. Wang, A. Kogan, D. Cobia, K. Alpert, A. Kolasny, M. I. Miller, D. Marcus, Northwestern university schizophrenia data and software tool (nusdast), Frontiers in neuroinformatics 7 (2013) 25. `doi:10.3389/fninf.2013.00025`.

[60] G. Sidhu, Locally linear embedding and fmri feature selection in psychiatric classification, IEEE journal of translational engineering in health and medicine 7 (2019) 1–11. `doi:10.1109/JTEHM.2019.2936348`.

[61] S. Potkin, J. Turner, G. Brown, G. McCarthy, D. Greve, G. Glover, D. Manoach, A. Belger, M. Diaz, C. Wible, et al., Working memory and dlpfc inefficiency in schizophrenia: the fbirn study, Schizophrenia bulletin 35 (1) (2009) 19–31. `doi:10.1093/schbul/sbn162`.

[62] G. Repovs, D. M. Barch, Working memory related brain network connectivity in individuals with schizophrenia and their siblings, Frontiers in human neuroscience 6 (2012) 137. `doi:10.3389/fnhum.2012.00137`.

[63] R. A. Poldrack, E. Congdon, W. Triplett, K. Gorgolewski, K. Karlsgodt, J. Mumford, F. Sabb, N. Freimer, E. London, T. Cannon, et al., A phenome-wide examination of neural and cognitive function, Scientific data 3 (1) (2016) 1–12. `doi:10.1038/sdata.2016.110`.

[64] https://www.kaggle.com/c/mlsp-2014-mri.

[65] M. Jenkinson, C. F. Beckmann, T. E. Behrens, M. W. Woolrich, S. M. Smith, Fsl, Neuroimage 62 (2) (2012) 782–790. `doi:10.1016/j.neuroimage.2011.09.015`.

[66] V. Popescu, M. Battaglini, W. Hoogstrate, S. C. Verfaillie, I. Sluimer, R. A. van Schijndel, B. W. van Dijk, K. S. Cover, D. L. Knol, M. Jenkinson, et al., Optimizing parameter choice for fsl-brain extraction tool (bet) on 3d t1 images in multiple sclerosis, Neuroimage 61 (4) (2012) 1484–1494. `doi:10.1016/j.neuroimage.2012.03.074`.

[67] B. Fischl, Freesurfer, Neuroimage 62 (2) (2012) 774–781. `doi:10.1016/j.neuroimage.2012.01.021`.

[68] J. Ashburner, Computational anatomy with the spm software, Magnetic resonance imaging 27 (8) (2009) 1163–1174. `doi:10.1016/j.mri.2009.01.006`.

[69] J. V. Manjón, Mri preprocessing, in: Imaging Biomarkers, Springer, 2017, pp. 53–63. `doi:10.1007/978-3-319-43504-6_5`.

[70] B.-y. Park, K. Byeon, H. Park, Funp (fusion of neuroimaging preprocessing) pipelines: a fully automated preprocessing software for functional magnetic resonance imaging, Frontiers in neuroinformatics 13 (2019) 5. `doi:10.3389/fninf.2019.00005`.

[71] I. Despotović, B. Goossens, W. Philips, Mri segmentation of the human brain: challenges, methods, and applications, Computational and mathematical methods in medicine 2015. `doi:10.1155/2015/450341`.

[72] S. Rajeshwari, T. S. Sharmila, Efficient quality analysis of mri image using preprocessing techniques, in: 2013 IEEE Conference on Information & Communication Technologies, IEEE, 2013, pp. 391–396. `doi:10.1109/CICT.2013.6558127`.

[73] E. B. George, M. Karnan, Mri brain image enhancement using filtering techniques, International Journal of Computer Science & Engineering Technology (IJCSET), ISSN (2012) 2229–3345.

[74] A. Pizurica, A. M. Wink, E. Vansteenkiste, W. Philips, B. J. Roerdink, A review of wavelet denoising in mri and ultrasound brain imaging, Current Medical Imaging 2 (2) (2006) 247–260. `doi:10.2174/157340506776930665`.

[75] H. A. Jaber, H. K. Aljobouri, İ. Çankaya, O. M. Koçak, O. Algin, Preparing fmri data for postprocessing: Conversion modalities, preprocessing pipeline, and parametric and nonparametric approaches, IEEE Access 7 (2019) 122864–122877. `doi:10.1109/ACCESS.2019.2937482`.

[76] M. Behroozi, M. R. Daliri, H. Boyaci, Statistical analysis methods for the fmri data, Basic and Clinical Neuroscience 2 (4) (2011) 67–74.

[77] B.-y. Park, K. Byeon, H. Park, Funp (fusion of neuroimaging preprocessing) pipelines: a fully automated preprocessing software for functional

magnetic resonance imaging, Frontiers in neuroinformatics 13 (2019) 5. `doi:10.3389/fninf.2019.00005`.

[78] N. Nabizadeh, M. Kubat, Brain tumors detection and segmentation in mr images: Gabor wavelet vs. statistical features, Computers & Electrical Engineering 45 (2015) 286–301. `doi:10.1016/j.compeleceng.2015.02.007`.

[79] M. Mohammadpoor, A. Shoeibi, H. Shojaee, et al., A hierarchical classification method for breast tumor detection, Iranian Journal of Medical Physics 13 (4) (2016) 261–268. `doi:10.22038/IJMP.2016.8453`.

[80] H. Zhuang, R. Liu, C. Wu, Z. Meng, D. Wang, D. Liu, M. Liu, Y. Li, Multimodal classification of drug-naïve first-episode schizophrenia combining anatomical, diffusion and resting state functional resonance imaging, Neuroscience letters 705 (2019) 87–93. `doi:10.1016/j.neulet.2019.04.039`.

[81] S. Han, Y. Wang, W. Liao, X. Duan, J. Guo, Y. Yu, L. Ye, J. Li, X. Chen, H. Chen, The distinguishing intrinsic brain circuitry in treatment-naïve first-episode schizophrenia: Ensemble learning classification, Neurocomputing 365 (2019) 44–53. `doi:10.1016/j.neucom.2019.07.061`.

[82] D. R. Gutierrez, A. Awwad, L. Meijer, M. Manita, T. Jaspan, R. A. Dineen, R. G. Grundy, D. P. Auer, Metrics and textural features of mri diffusion to improve classification of pediatric posterior fossa tumors, American Journal of Neuroradiology 35 (5) (2014) 1009–1015. `doi:10.3174/ajnr.A3784`.

[83] P. Georgiadis, D. Cavouras, I. Kalatzis, A. Daskalakis, G. C. Kagadis, K. Sifaki, M. Malamas, G. Nikiforidis, E. Solomou, Improving brain tumor characterization on mri by probabilistic neural networks and non-linear transformation of textural features, Computer methods and programs in biomedicine 89 (1) (2008) 24–32. `doi:10.1016/j.cmpb.2007.10.007`.

[84] M. Partio, B. Cramariuc, M. Gabbouj, A. Visa, Rock texture retrieval using gray level co-occurrence matrix, in: Proc. of 5th Nordic Signal Processing Symposium, Vol. 75, Citeseer, 2002.

[85] S. Jafarpour, Z. Sedghi, M. C. Amirani, A robust brain mri classification with glcm features, International Journal of Computer Applications 37 (12) (2012) 1–5. doi:10.5120/4735-6872.

[86] A. K. Singh, R. Singla, et al., Different approaches of classification of brain tumor in mri using gabor filters for feature extraction, in: Soft Computing: Theories and Applications, Springer, 2020, pp. 1175–1188. doi:10.1007/978-981-15-0751-9_108.

[87] G. Gilanie, U. I. Bajwa, M. M. Waraich, Z. Habib, H. Ullah, M. Nasir, Classification of normal and abnormal brain mri slices using gabor texture and support vector machines, Signal, Image and Video Processing 12 (3) (2018) 479–487. doi:10.1007/s11760-017-1182-8.

[88] W. Yu, Z. Na, Y. Fengxia, G. Yanping, Magnetic resonance imaging study of gray matter in schizophrenia based on xgboost, Journal of Integrative Neuroscience 17 (4) (2018) 331–336. doi:10.31083/j.jin.2018.04.0410.

[89] S. Sartipi, H. Kalbkhani, M. G. Shayesteh, Diagnosis of schizophrenia from r-fmri data using ripplet transform and olpp, Multimedia Tools and Applications 79 (2020) 23401–23423. doi:10.1007/s11042-020-09122-y.

[90] U. R. Acharya, S. V. Sree, P. C. A. Ang, R. Yanti, J. S. Suri, Application of non-linear and wavelet based features for the automated identification of epileptic eeg signals, International journal of neural systems 22 (02) (2012) 1250002. doi:10.1142/S0129065712500025.

[91] A. Juneja, B. Rana, R. Agrawal, A novel fuzzy rough selection of non-linearly extracted features for schizophrenia diagnosis using fmri, Com-

puter methods and programs in biomedicine 155 (2018) 139–152. `doi:10.1016/j.cmpb.2017.12.001`.

[92] T.-W. Lee, S.-W. Xue, Linking graph features of anatomical architecture to regional brain activity: A multi-modal mri study, Neuroscience letters 651 (2017) 123–127. `doi:10.1016/j.neulet.2017.05.005`.

[93] A. Messé, G. Marrelec, P. Bellec, V. Perlbarg, J. Doyon, M. Pélégrini-Issac, H. Benali, Comparing structural and functional graph theory features in the human brain using multimodal mri, Irbm 33 (4) (2012) 244–253. `doi:10.1016/j.irbm.2012.04.005`.

[94] R. F. Algunaid, A. H. Algumaei, M. A. Rushdi, I. A. Yassine, Schizophrenic patient identification using graph-theoretic features of resting-state fmri data, Biomedical Signal Processing and Control 43 (2018) 289–299. `doi:10.1016/j.bspc.2018.02.018`.

[95] Y. Xiang, J. Wang, G. Tan, F.-X. Wu, J. Liu, Schizophrenia identification using multi-view graph measures of functional brain networks, Frontiers in bioengineering and biotechnology 7 (2020) 479. `doi:10.3389/fbioe.2019.00479`.

[96] S. H. Hojjati, A. Ebrahimzadeh, A. Khazaee, A. Babajani-Feremi, A. D. N. Initiative, et al., Predicting conversion from mci to ad by integrating rs-fmri and structural mri, Computers in biology and medicine 102 (2018) 30–39. `doi:10.1016/j.compbiomed.2018.09.004`.

[97] S. Sargolzaei, M. Cabrerizo, M. Goryawala, A. S. Eddin, M. Adjouadi, Scalp eeg brain functional connectivity networks in pediatric epilepsy, Computers in biology and medicine 56 (2015) 158–166. `doi:10.1016/j.compbiomed.2014.10.018`.

[98] B. P. Rogers, V. L. Morgan, A. T. Newton, J. C. Gore, Assessing functional connectivity in the human brain by fmri, Magnetic resonance imaging 25 (10) (2007) 1347–1357. `doi:10.1016/j.mri.2007.03.007`.

[99] R. Meszlényi, L. Peska, V. Gál, Z. Vidnyánszky, K. Buza, Classification of fmri data using dynamic time warping based functional connectivity analysis, in: 2016 24th European signal processing conference (EUSIPCO), IEEE, 2016, pp. 245–249. `doi:10.1109/EUSIPCO.2016.7760247`.

[100] C.-H. Yeh, D. K. Jones, X. Liang, M. Descoteaux, A. Connelly, Mapping structural connectivity using diffusion mri: Challenges and opportunities, Journal of Magnetic Resonance Imaging`doi:10.1002/jmri.27188`.

[101] B. Mwangi, T. S. Tian, J. C. Soares, A review of feature reduction techniques in neuroimaging, Neuroinformatics 12 (2) (2014) 229–244. `doi:10.1007/s12021-013-9204-3`.

[102] A. Jović, K. Brkić, N. Bogunović, A review of feature selection methods with applications, in: 2015 38th international convention on information and communication technology, electronics and microelectronics (MIPRO), Ieee, 2015, pp. 1200–1205. `doi:10.1109/MIPRO.2015.7160458`.

[103] V. Kumar, S. Minz, Feature selection: a literature review, SmartCR 4 (3) (2014) 211–229.

[104] S. Wold, K. Esbensen, P. Geladi, Principal component analysis, Chemometrics and intelligent laboratory systems 2 (1-3) (1987) 37–52. `doi:10.1016/0169-7439(87)80084-9`.

[105] S. H. Huang, Supervised feature selection: A tutorial., Artif. Intell. Research 4 (2) (2015) 22–37.

[106] S. Solorio-Fernández, J. A. Carrasco-Ochoa, J. F. Martínez-Trinidad, A review of unsupervised feature selection methods, Artificial Intelligence Review 53 (2) (2020) 907–948. `doi:10.1007/s10462-019-09682-y`.

[107] Q. Al-Tashi, H. M. Rais, S. J. Abdulkadir, S. Mirjalili, H. Alhussian, A review of grey wolf optimizer-based feature selection methods for classi-

fication, Evolutionary Machine Learning Techniques (2020) 273–286`doi:`
`10.1007/978-981-32-9990-0_13`.

[108] R. J. Urbanowicz, M. Meeker, W. La Cava, R. S. Olson, J. H. Moore, Relief-based feature selection: Introduction and review, Journal of biomedical informatics 85 (2018) 189–203. `doi:10.1016/j.jbi.2018.` `07.014`.

[109] Q. Gu, Z. Li, J. Han, Generalized fisher score for feature selection, arXiv preprint arXiv:1202.3725.

[110] A. W. Haryanto, E. K. Mawardi, et al., Influence of word normalization and chi-squared feature selection on support vector machine (svm) text classification, in: 2018 International Seminar on Application for Technology of Information and Communication, IEEE, 2018, pp. 229–233. `doi:10.1109/ISEMANTIC.2018.8549748`.

[111] M. A. Hall, Correlation-based feature selection for machine learning.

[112] Y. Bae, K. Kumarasamy, I. M. Ali, P. Korfiatis, Z. Akkus, B. J. Erickson, Differences between schizophrenic and normal subjects using network properties from fmri, Journal of digital imaging 31 (2) (2018) 252–261. `doi:10.1007/s10278-017-0020-4`.

[113] X.-L. Cai, D.-J. Xie, K. H. Madsen, Y.-M. Wang, S. A. Bögemann, E. F. Cheung, A. Møller, R. C. Chan, Generalizability of machine learning for classification of schizophrenia based on resting-state functional mri data, Human brain mapping 41 (1) (2020) 172–184. `doi:10.1002/hbm.24797`.

[114] J. Yang, W. Pu, G. Wu, E. Chen, E. Lee, Z. Liu, L. Palaniyappan, Connectomic underpinnings of working memory deficits in schizophrenia: Evidence from a replication fmri study, Schizophrenia bulletin 46 (4) (2020) 916–926. `doi:10.1093/schbul/sbz137`.

[115] S. Wang, Y. Zhan, Y. Zhang, L. Lyu, H. Lyu, G. Wang, R. Wu, J. Zhao, W. Guo, Abnormal long-and short-range functional connec-

tivity in adolescent-onset schizophrenia patients: a resting-state fmri study, Progress in Neuro-Psychopharmacology and Biological Psychiatry 81 (2018) 445–451. `doi:10.1016/j.pnpbp.2017.08.012`.

[116] P. Mitra, C. Murthy, S. K. Pal, Unsupervised feature selection using feature similarity, IEEE transactions on pattern analysis and machine intelligence 24 (3) (2002) 301–312. `doi:10.1109/34.990133`.

[117] B. Venkatesh, J. Anuradha, A review of feature selection and its methods, Cybernetics and Information Technologies 19 (1) (2019) 3–26. `doi:10.2478/cait-2019-0001`.

[118] A. A. Pandit, B. Pimpale, S. Dubey, A comprehensive review on unsupervised feature selection algorithms, in: International Conference on Intelligent Computing and Smart Communication 2019, Springer, 2020, pp. 255–266. `doi:10.1007/978-981-15-0633-8_24`.

[119] Y. Saeys, I. Inza, P. Larranaga, A review of feature selection techniques in bioinformatics, bioinformatics 23 (19) (2007) 2507–2517. `doi:10.1093/bioinformatics/btm344`.

[120] A. Talpalaru, N. Bhagwat, G. A. Devenyi, M. Lepage, M. M. Chakravarty, Identifying schizophrenia subgroups using clustering and supervised learning, Schizophrenia research 214 (2019) 51–59. `doi:10.1016/j.schres.2019.05.044`.

[121] I.-S. Oh, J.-S. Lee, B.-R. Moon, Hybrid genetic algorithms for feature selection, IEEE Transactions on pattern analysis and machine intelligence 26 (11) (2004) 1424–1437. `doi:10.1109/TPAMI.2004.105`.

[122] O. H. Babatunde, L. Armstrong, J. Leng, D. Diepeveen, A genetic algorithm-based feature selection.

[123] M. M. Kabir, M. Shahjahan, K. Murase, A new hybrid ant colony optimization algorithm for feature selection, Expert Systems with Applications 39 (3) (2012) 3747–3763. `doi:10.1016/j.eswa.2011.09.073`.

[124] İ. Babaoglu, O. Findik, E. Ülker, A comparison of feature selection models utilizing binary particle swarm optimization and genetic algorithm in determining coronary artery disease using support vector machine, Expert Systems with Applications 37 (4) (2010) 3177–3183. `doi:10.1016/j.eswa.2009.09.064`.

[125] T. M. Hamdani, J.-M. Won, A. M. Alimi, F. Karray, Multi-objective feature selection with nsga ii, in: International conference on adaptive and natural computing algorithms, Springer, 2007, pp. 240–247. `doi:10.1007/978-3-540-71618-1_27`.

[126] S. Laksshman, R. R. Bhat, V. Viswanath, X. Li, Deepbipolar: Identifying genomic mutations for bipolar disorder via deep learning, Human mutation 38 (9) (2017) 1217–1224. `doi:10.1002/humu.23272`.

[127] Q. Sun, Q. Yue, F. Zhu, K. Shu, The identification research of bipolar disorder based on cnn, in: Journal of Physics: Conference Series, Vol. 1168, IOP Publishing, 2019, p. 032125.

[128] Y. Mehta, N. Majumder, A. Gelbukh, E. Cambria, Recent trends in deep learning based personality detection, Artificial Intelligence Review (2019) 1–27`doi:10.1007/s10462-019-09770-z`.

[129] M. Pominova, A. Artemov, M. Sharaev, E. Kondrateva, A. Bernstein, E. Burnaev, Voxelwise 3d convolutional and recurrent neural networks for epilepsy and depression diagnostics from structural and functional mri data, in: 2018 IEEE International Conference on Data Mining Workshops (ICDMW), IEEE, 2018, pp. 299–307. `doi:10.1109/ICDMW.2018.00050`.

[130] W. H. Pinaya, A. Mechelli, J. R. Sato, Using deep autoencoders to identify abnormal brain structural patterns in neuropsychiatric disorders: A large-scale multi-sample study, Human brain mapping 40 (3) (2019) 944–954. `doi:10.1002/hbm.24423`.

[131] A. Gulli, S. Pal, Deep learning with Keras, Packt Publishing Ltd, 2017.

[132] M. A. Nielsen, Neural networks and deep learning, Vol. 25, Determination press San Francisco, CA, 2015.

[133] D. Shen, G. Wu, H.-I. Suk, Deep learning in medical image analysis, Annual review of biomedical engineering 19 (2017) 221–248. `doi:/10.1146/annurev-bioeng-071516-044442`.

[134] I. Goodfellow, Y. Bengio, A. Courville, Y. Bengio, Deep learning, Vol. 1, MIT press Cambridge, 2016.

[135] Y. LeCun, Y. Bengio, G. Hinton, Deep learning, nature 521 (7553) (2015) 436–444. `doi:10.1038/nature14539`.

[136] I. J. Goodfellow, J. Pouget-Abadie, M. Mirza, B. Xu, D. Warde-Farley, S. Ozair, A. Courville, Y. Bengio, Generative adversarial networks, arXiv preprint arXiv:1406.2661.

[137] N. Ghassemi, H. Mahami, M. T. Darbandi, A. Shoeibi, S. Hussain, F. Nasirzadeh, R. Alizadehsani, D. Nahavandi, A. Khosravi, S. Nahavandi, Material recognition for automated progress monitoring using deep learning methods, arXiv preprint arXiv:2006.16344.

[138] K. Simonyan, A. Zisserman, Very deep convolutional networks for large-scale image recognition, arXiv preprint arXiv:1409.1556.

[139] A. Shoeibi, N. Ghassemi, M. Khodatars, M. Jafari, S. Hussain, R. Alizadehsani, P. Moridian, A. Khosravi, H. Hosseini-Nejad, M. Rouhani, et al., Epileptic seizure detection using deep learning techniques: A review, arXiv preprint arXiv:2007.01276.

[140] C. Szegedy, W. Liu, Y. Jia, P. Sermanet, S. Reed, D. Anguelov, D. Erhan, V. Vanhoucke, A. Rabinovich, Going deeper with convolutions, in: Proceedings of the IEEE conference on computer vision and pattern recognition, 2015, pp. 1–9.

[141] G. C. Jana, R. Sharma, A. Agrawal, A 1d-cnn-spectrogram based approach for seizure detection from eeg signal, Procedia Computer Science 167 (2020) 403–412. `doi:10.1016/j.procs.2020.03.248`.

[142] C. Szegedy, S. Ioffe, V. Vanhoucke, A. Alemi, Inception-v4, inception-resnet and the impact of residual connections on learning, in: Proceedings of the AAAI Conference on Artificial Intelligence, Vol. 31, 2017.

[143] A. Creswell, T. White, V. Dumoulin, K. Arulkumaran, B. Sengupta, A. A. Bharath, Generative adversarial networks: An overview, IEEE Signal Processing Magazine 35 (1) (2018) 53–65. `doi:10.1109/MSP.2017.2765202`.

[144] N. Ghassemi, A. Shoeibi, M. Rouhani, Deep neural network with generative adversarial networks pre-training for brain tumor classification based on mr images, Biomedical Signal Processing and Control 57 (2020) 101678. `doi:10.1016/j.bspc.2019.101678`.

[145] S. Sabour, N. Frosst, G. E. Hinton, Dynamic routing between capsules, arXiv preprint arXiv:1710.09829.

[146] R. Mukhometzianov, J. Carrillo, Capsnet comparative performance evaluation for image classification, arXiv preprint arXiv:1805.11195.

[147] S. P. Singh, L. Wang, S. Gupta, H. Goli, P. Padmanabhan, B. Gulyás, 3d deep learning on medical images: a review, Sensors 20 (18) (2020) 5097. `doi:10.3390/s20185097`.

[148] A. Shoeibi, M. Khodatars, R. Alizadehsani, N. Ghassemi, M. Jafari, P. Moridian, A. Khadem, D. Sadeghi, S. Hussain, A. Zare, et al., Automated detection and forecasting of covid-19 using deep learning techniques: A review, arXiv preprint arXiv:2007.10785.

[149] J. Zabalza, J. Ren, J. Zheng, H. Zhao, C. Qing, Z. Yang, P. Du, S. Marshall, Novel segmented stacked autoencoder for effective dimensionality reduction and feature extraction in hyperspectral imaging, Neurocomputing 185 (2016) 1–10. `doi:10.1016/j.neucom.2015.11.044`.

[150] A. Majumdar, Blind denoising autoencoder, IEEE transactions on neural networks and learning systems 30 (1) (2018) 312–317. `doi:10.1109/TNNLS.2018.2838679`.

[151] A. Ng, et al., Sparse autoencoder, CS294A Lecture notes 72 (2011) (2011) 1–19.

[152] Y. Hu, Y. Wong, W. Wei, Y. Du, M. Kankanhalli, W. Geng, A novel attention-based hybrid cnn-rnn architecture for semg-based gesture recognition, PloS one 13 (10) (2018) e0206049. `doi:10.1371/journal.pone.0206049`.

[153] X. Zhu, L. Li, W. Zhang, T. Rao, M. Xu, Q. Huang, D. Xu, Dependency exploitation: A unified cnn-rnn approach for visual emotion recognition, in: proceedings of the 26th international joint conference on artificial intelligence, 2017, pp. 3595–3601.

[154] K. P. Bennett, J. Blue, A support vector machine approach to decision trees, in: 1998 IEEE International Joint Conference on Neural Networks Proceedings. IEEE World Congress on Computational Intelligence (Cat. No. 98CH36227), Vol. 3, IEEE, 1998, pp. 2396–2401. `doi:10.1109/IJCNN.1998.687237`.

[155] T. Joachims, Svmlight: Support vector machine, SVM-Light Support Vector Machine http://svmlight. joachims. org/, University of Dortmund 19 (4).

[156] M. Pal, Random forest classifier for remote sensing classification, International journal of remote sensing 26 (1) (2005) 217–222. `doi:10.1080/01431160412331269698`.

[157] F. Zang, J.-s. Zhang, Softmax discriminant classifier, in: 2011 Third International Conference on Multimedia Information Networking and Security, IEEE, 2011, pp. 16–19. `doi:10.1109/MINES.2011.123`.

[158] M. Mirjalili, G.-A. Hossein-Zadeh, Characterization of schizophrenia by linear kernel canonical correlation analysis of resting-state functional mri and structural mri, in: 2017 7th International Conference on Computer and Knowledge Engineering (ICCKE), IEEE, 2017, pp. 37–41. `doi:10.1109/ICCKE.2017.8167925`.

[159] M. S. Salman, Y. Du, V. D. Calhoun, Identifying fmri dynamic connectivity states using affinity propagation clustering method: Application to schizophrenia, in: 2017 IEEE International Conference on Acoustics, Speech and Signal Processing (ICASSP), IEEE, 2017, pp. 904–908. `doi:10.1109/ICASSP.2017.7952287`.

[160] P. Liu, X. Mei, S. Fei, A compound classification model for schizophrenia based on brain fmri and network modelling, in: 2019 Chinese Control Conference (CCC), IEEE, 2019, pp. 7694–7697. `doi:10.23919/ChiCC.2019.8865960`.

[161] S. Wang, Y. Zhang, L. Lv, R. Wu, X. Fan, J. Zhao, W. Guo, Abnormal regional homogeneity as a potential imaging biomarker for adolescent-onset schizophrenia: a resting-state fmri study and support vector machine analysis, Schizophrenia research 192 (2018) 179–184. `doi:10.1016/j.schres.2017.05.038`.

[162] Y. Xiao, Z. Yan, Y. Zhao, B. Tao, H. Sun, F. Li, L. Yao, W. Zhang, S. Chandan, J. Liu, et al., Support vector machine-based classification of first episode drug-naïve schizophrenia patients and healthy controls using structural mri, Schizophrenia Research 214 (2019) 11–17. `doi:10.1016/j.schres.2017.11.037`.

[163] J. Hua, N. I. Blair, A. Paez, A. Choe, A. D. Barber, A. Brandt, I. A. L. Lim, F. Xu, V. Kamath, J. J. Pekar, et al., Altered functional connectivity between sub-regions in the thalamus and cortex in schizophrenia patients measured by resting state bold fmri at 7t, Schizophrenia research 206 (2019) 370–377. `doi:10.1016/j.schres.2018.10.016`.

[164] E. Kirino, S. Tanaka, M. Fukuta, R. Inami, H. Arai, R. Inoue, S. Aoki, Simultaneous resting-state functional mri and electroencephalography recordings of functional connectivity in patients with schizophrenia, Psychiatry and clinical neurosciences 71 (4) (2017) 262–270. `doi:10.1111/pcn.12495`.

[165] X. Lu, Y. Yang, F. Wu, M. Gao, Y. Xu, Y. Zhang, Y. Yao, X. Du, C. Li, L. Wu, et al., Discriminative analysis of schizophrenia using support vector machine and recursive feature elimination on structural mri images, Medicine 95 (30). `doi:10.1097/MD.0000000000003973`.

[166] A. Juneja, B. Rana, R. Agrawal, A combination of singular value decomposition and multivariate feature selection method for diagnosis of schizophrenia using fmri, Biomedical Signal Processing and Control 27 (2016) 122–133. `doi:10.1016/j.bspc.2016.02.009`.

[167] Q. Zhu, J. Huang, X. Xu, Non-negative discriminative brain functional connectivity for identifying schizophrenia on resting-state fmri, Biomedical engineering online 17 (1) (2018) 1–15. `doi:10.1186/s12938-018-0464-x`.

[168] P. Moghimi, K. O. Lim, T. I. Netoff, Data driven classification using fmri network measures: application to schizophrenia, Frontiers in neuroinformatics 12 (2018) 71. `doi:10.3389/fninf.2018.00071`.

[169] M. S. Cetin, J. M. Houck, B. Rashid, O. Agacoglu, J. M. Stephen, J. Sui, J. Canive, A. Mayer, C. Aine, J. R. Bustillo, et al., Multimodal classification of schizophrenia patients with meg and fmri data using static and dynamic connectivity measures, Frontiers in neuroscience 10 (2016) 466. `doi:doi.org/10.3389/fnins.2016.00466`.

[170] I. Chatterjee, M. Agarwal, B. Rana, N. Lakhyani, N. Kumar, Bi-objective approach for computer-aided diagnosis of schizophrenia patients using fmri data, Multimedia Tools and Applications 77 (20) (2018) 26991–27015. `doi:10.1007/s11042-018-5901-0`.

[171] M. Latha, G. Kavitha, Segmentation and texture analysis of structural biomarkers using neighborhood-clustering-based level set in mri of the schizophrenic brain, Magnetic Resonance Materials in Physics, Biology and Medicine 31 (4) (2018) 483–499. `doi:10.1007/s10334-018-0674-z`.

[172] M. Singh, R. Badhwar, G. Bagler, Graph theoretical biomarkers for schizophrenic brain functional networks, in: 2016 International Conference on Signal Processing and Communication (ICSC), IEEE, 2016, pp. 289–294. `doi:10.1109/ICSPCom.2016.7980593`.

[173] A. V. Nimkar, D. R. Kubal, Optimization of schizophrenia diagnosis prediction using machine learning techniques, in: 2018 4th International Conference on Computer and Information Sciences (ICCOINS), IEEE, 2018, pp. 1–6. `doi:10.1109/ICCOINS.2018.8510599`.

[174] M. S. Sendi, E. Zendehrouh, Z. Fu, B. Mahmoudi, R. L. Miller, V. D. Calhoun, A machine learning model for exploring aberrant functional network connectivity transition in schizophrenia, in: 2020 IEEE Southwest Symposium on Image Analysis and Interpretation (SSIAI), IEEE, 2020, pp. 112–115. `doi:10.1109/SSIAI49293.2020.9094620`.

[175] A. F. Rodrigues, M. Barros, P. Furtado, Squizofrenia: Classification and correlation from mri, in: 2017 IEEE EMBS International Conference on Biomedical & Health Informatics (BHI), IEEE, 2017, pp. 381–384. `doi:10.1109/BHI.2017.7897285`.

[176] X. Mei, W. Li, R. Chellali, Y. Zhou, J. Huang, S. Ma, Nodes-weighted-graph approach for rsfmri data classification: Application to schizophrenia, in: 2016 35th Chinese Control Conference (CCC), IEEE, 2016, pp. 3962–3966. `doi:10.1109/ChiCC.2016.7553971`.

[177] Y. Yang, Y. Cui, K. Xu, B. Liu, M. Song, J. Chen, H. Wang, Y. Chen, H. Guo, P. Li, et al., Distributed functional connectivity impairment in schizophrenia: a multi-site study`doi:10.1049/cp.2017.0086`.

[178] K. Dillon, Y.-P. Wang, An image resolution perspective on functional activity mapping, in: 2016 38th Annual International Conference of the IEEE Engineering in Medicine and Biology Society (EMBC), IEEE, 2016, pp. 1139–1142. `doi:10.1109/EMBC.2016.7590905`.

[179] J. Su, H. Shen, L.-L. Zeng, J. Qin, Z. Liu, D. Hu, Heredity characteristics of schizophrenia shown by dynamic functional connectivity analysis of resting-state functional mri scans of unaffected siblings, Neuroreport 27 (11) (2016) 843–848. `doi:10.1097/WNR.0000000000000622`.

[180] L. Yuan, T. Liu, D. Hu, Group-wise sparse representation of resting-state fmri data for better understanding of schizophrenia, in: 2017 IEEE 14th International Symposium on Biomedical Imaging (ISBI 2017), IEEE, 2017, pp. 952–956. `doi:10.1109/ISBI.2017.7950673`.

[181] J. Huang, Q. Zhu, X. Hao, X. Shi, S. Gao, X. Xu, D. Zhang, Identifying resting-state multifrequency biomarkers via tree-guided group sparse learning for schizophrenia classification, IEEE journal of biomedical and health informatics 23 (1) (2018) 342–350. `doi:10.1109/JBHI.2018.2796588`.

[182] F. Yamashita, M. Sasaki, K. Fukumoto, K. Otsuka, I. Uwano, H. Kameda, J. Endoh, A. Sakai, Detection of changes in the ventral tegmental area of patients with schizophrenia using neuromelanin-sensitive mri, Neuroreport 27 (5) (2016) 289–294. `doi:10.1097/WNR.0000000000000530`.

[183] E. Acar, Y. Levin-Schwartz, V. D. Calhoun, T. Adali, Tensor-based fusion of eeg and fmri to understand neurological changes in schizophrenia, in: 2017 IEEE International Symposium on Circuits and Systems (ISCAS), IEEE, 2017, pp. 1–4. `doi:10.1109/ISCAS.2017.8050303`.

[184] A. de Pierrefeu, T. Löfstedt, C. Laidi, F. Hadj-Selem, M. Leboyer, P. Ciuciu, J. Houenou, E. Duchesnay, Interpretable and stable prediction of schizophrenia on a large multisite dataset using machine learn-

ing with structured sparsity, in: 2018 International Workshop on Pattern Recognition in Neuroimaging (PRNI), IEEE, 2018, pp. 1–4. `doi:10.1109/PRNI.2018.8423946`.

[185] R. L. Miller, V. D. Calhoun, Dynamic whole brain polarity regimes strongly distinguish controls from schizophrenia patients, in: 2018 International Workshop on Pattern Recognition in Neuroimaging (PRNI), IEEE, 2018, pp. 1–4. `doi:10.1109/PRNI.2018.8423965`.

[186] W. Hu, D. Lin, V. D. Calhoun, Y.-p. Wang, Integration of snps-fmri-methylation data with sparse multi-cca for schizophrenia study, in: 2016 38th Annual International Conference of the IEEE Engineering in Medicine and Biology Society (EMBC), IEEE, 2016, pp. 3310–3313. `doi:10.1109/EMBC.2016.7591436`.

[187] E. Zarogianni, A. J. Storkey, E. C. Johnstone, D. G. Owens, S. M. Lawrie, Improved individualized prediction of schizophrenia in subjects at familial high risk, based on neuroanatomical data, schizotypal and neurocognitive features, Schizophrenia Research 181 (2017) 6–12. `doi:10.1016/j.schres.2016.08.027`.

[188] K. Dontaraju, S.-J. Kim, M. Akhonda, T. Adali, Capturing common and individual components in fmri data by discriminative dictionary learning, in: 2018 52nd Asilomar Conference on Signals, Systems, and Computers, IEEE, 2018, pp. 1351–1356. `doi:10.1109/ACSSC.2018.8645300`.

[189] J. L. Winterburn, A. N. Voineskos, G. A. Devenyi, E. Plitman, C. de la Fuente-Sandoval, N. Bhagwat, A. Graff-Guerrero, J. Knight, M. M. Chakravarty, Can we accurately classify schizophrenia patients from healthy controls using magnetic resonance imaging and machine learning? a multi-method and multi-dataset study, Schizophrenia research 214 (2019) 3–10. `doi:10.1016/j.schres.2017.11.038`.

[190] J. Lee, M.-W. Chon, H. Kim, Y. Rathi, S. Bouix, M. E. Shenton,

M. Kubicki, Diagnostic value of structural and diffusion imaging measures in schizophrenia, NeuroImage: Clinical 18 (2018) 467–474. `doi:10.1016/j.nicl.2018.02.007`.

[191] S. Liang, W. Deng, X. Li, Q. Wang, A. J. Greenshaw, W. Guo, X. Kong, M. Li, L. Zhao, Y. Meng, et al., Aberrant posterior cingulate connectivity classify first-episode schizophrenia from controls: A machine learning study, Schizophrenia research 220 (2020) 187–193. `doi:10.1016/j.schres.2020.03.022`.

[192] Y. Liu, Y. Zhang, L. Lv, R. Wu, J. Zhao, W. Guo, Abnormal neural activity as a potential biomarker for drug-naive first-episode adolescent-onset schizophrenia with coherence regional homogeneity and support vector machine analyses, Schizophrenia research 192 (2018) 408–415. `doi:10.1016/j.schres.2017.04.028`.

[193] L. Liu, L.-B. Cui, X.-S. Wu, N.-B. Fei, Z.-L. Xu, D. Wu, Y.-B. Xi, P. Huang, K. M. von Deneen, S. Qi, et al., Cortical abnormalities and identification for first-episode schizophrenia via high-resolution magnetic resonance imaging, Biomarkers in Neuropsychiatry 3 (2020) 100022. `doi:10.1016/j.bionps.2020.100022`.

[194] Y. Deng, K. S. Hung, S. S. Lui, W. W. Chui, J. C. Lee, Y. Wang, Z. Li, H. K. Mak, P. C. Sham, R. C. Chan, et al., Tractography-based classification in distinguishing patients with first-episode schizophrenia from healthy individuals, Progress in Neuro-Psychopharmacology and Biological Psychiatry 88 (2019) 66–73. `doi:10.1016/j.pnpbp.2018.06.010`.

[195] J. Liu, X. Wang, X. Zhang, Y. Pan, X. Wang, J. Wang, Mmm: classification of schizophrenia using multi-modality multi-atlas feature representation and multi-kernel learning, Multimedia Tools and Applications 77 (22) (2018) 29651–29667. `doi:10.1007/s11042-017-5470-7`.

[196] L. Manohar, K. Ganesan, Diagnosis of schizophrenia disorder in mr brain images using multi-objective bpso based feature selection with fuzzy svm,

Journal of Medical and Biological Engineering 38 (6) (2018) 917–932. `doi: 10.1007/s40846-017-0355-9`.

[197] C. Tas, H. Mogulkoc, G. Eryilmaz, I. Gogcegoz-Gul, T. T. Erguzel, B. Metin, N. K. Tarhan, Discriminating schizophrenia and schizo-obsessive disorder: a structural mri study combining vbm and machine learning methods, Neural Computing and Applications 29 (2) (2018) 377–387. `doi:10.1007/s00521-016-2451-0`.

[198] Z. Chen, T. Yan, E. Wang, H. Jiang, Y. Tang, X. Yu, J. Zhang, C. Liu, Detecting abnormal brain regions in schizophrenia using structural mri via machine learning, Computational intelligence and neuroscience 2020. `doi:10.1155/2020/6405930`.

[199] I. Chatterjee, V. Kumar, B. Rana, M. Agarwal, N. Kumar, Impact of ageing on the brain regions of the schizophrenia patients: an fmri study using evolutionary approach, Multimedia Tools and Applications 79 (33) (2020) 24757–24779. `doi:10.1007/s11042-020-09183-z`.

[200] A. Juneja, B. Rana, R. Agrawal, fmri based computer aided diagnosis of schizophrenia using fuzzy kernel feature extraction and hybrid feature selection, Multimedia Tools and Applications 77 (3) (2018) 3963–3989. `doi:10.1007/s11042-017-4404-8`.

[201] A. M. de Moura, W. H. L. Pinaya, A. Gadelha, A. Zugman, C. Noto, Q. Cordeiro, S. I. Belangero, A. P. Jackowski, R. A. Bressan, J. R. Sato, Investigating brain structural patterns in first episode psychosis and schizophrenia using mri and a machine learning approach, Psychiatry Research: Neuroimaging 275 (2018) 14–20. `doi:10.1016/j.pscychresns.2018.03.003`.

[202] H. Zou, J. Yang, Multiple functional connectivity networks fusion for schizophrenia diagnosis, Medical & biological engineering & computing 58 (2020) 1779–1790. `doi:10.1007/s11517-020-02193-x`.

[203] M. A. Alam, H.-Y. Lin, H.-W. Deng, V. D. Calhoun, Y.-P. Wang, A kernel machine method for detecting higher order interactions in multimodal datasets: Application to schizophrenia, Journal of neuroscience methods 309 (2018) 161–174. `doi:10.1016/j.jneumeth.2018.08.027`.

[204] J. Chen, K. R. Patil, S. Weis, K. Sim, T. Nickl-Jockschat, J. Zhou, A. Aleman, I. E. Sommer, E. J. Liemburg, F. Hoffstaedter, et al., Neurobiological divergence of the positive and negative schizophrenia subtypes identified on a new factor structure of psychopathology using non-negative factorization: An international machine learning study, Biological psychiatry 87 (3) (2020) 282–293. `doi:doi.org/10.1016/j.biopsych.2019.08.031`.

[205] Y. Guo, J. Qiu, W. Lu, Support vector machine-based schizophrenia classification using morphological information from amygdaloid and hippocampal subregions, Brain Sciences 10 (8) (2020) 562. `doi:10.3390/brainsci10080562`.

[206] Y. Pan, W. Pu, X. Chen, X. Huang, Y. Cai, H. Tao, Z. Xue, M. Mackinley, R. Limongi, Z. Liu, et al., Morphological profiling of schizophrenia: cluster analysis of mri-based cortical thickness data, Schizophrenia bulletin 46 (3) (2020) 623–632. `doi:10.1093/schbul/sbz112`.

[207] D. B. Dwyer, C. Cabral, L. Kambeitz-Ilankovic, R. Sanfelici, J. Kambeitz, V. Calhoun, P. Falkai, C. Pantelis, E. Meisenzahl, N. Koutsouleris, Brain subtyping enhances the neuroanatomical discrimination of schizophrenia, Schizophrenia bulletin 44 (5) (2018) 1060–1069. `doi:10.1093/schbul/sby008`.

[208] P. Orban, C. Dansereau, L. Desbois, V. Mongeau-Pérusse, C.-É. Giguère, H. Nguyen, A. Mendrek, E. Stip, P. Bellec, Multisite generalizability of schizophrenia diagnosis classification based on functional brain connectivity, Schizophrenia research 192 (2018) 167–171. `doi:10.1016/j.schres.2017.05.027`.

[209] S. Ramkiran, A. Sharma, N. P. Rao, Resting-state anticorrelated networks in schizophrenia, Psychiatry Research: Neuroimaging 284 (2019) 1–8. `doi:10.1016/j.pscychresns.2018.12.013`.

[210] R. Jing, P. Li, Z. Ding, X. Lin, R. Zhao, L. Shi, H. Yan, J. Liao, C. Zhuo, L. Lu, et al., Machine learning identifies unaffected first-degree relatives with functional network patterns and cognitive impairment similar to those of schizophrenia patients, Human brain mapping 40 (13) (2019) 3930–3939. `doi:10.1002/hbm.24678`.

[211] M. N. I. Qureshi, J. Oh, D. Cho, H. J. Jo, B. Lee, Multimodal discrimination of schizophrenia using hybrid weighted feature concatenation of brain functional connectivity and anatomical features with an extreme learning machine, Frontiers in neuroinformatics 11 (2017) 59. `doi:10.3389/fninf.2017.00059`.

[212] F. Zhu, Y. Liu, F. Liu, R. Yang, H. Li, J. Chen, D. N. Kennedy, J. Zhao, W. Guo, Functional asymmetry of thalamocortical networks in subjects at ultra-high risk for psychosis and first-episode schizophrenia, European Neuropsychopharmacology 29 (4) (2019) 519–528. `doi:10.1016/j.euroneuro.2019.02.006`.

[213] J. Li, Y. Sun, Y. Huang, A. Bezerianos, R. Yu, Machine learning technique reveals intrinsic characteristics of schizophrenia: an alternative method, Brain imaging and behavior 13 (5) (2019) 1386–1396. `doi:10.1007/s11682-018-9947-4`.

[214] W. Guo, F. Liu, J. Chen, R. Wu, L. Li, Z. Zhang, H. Chen, J. Zhao, Using short-range and long-range functional connectivity to identify schizophrenia with a family-based case-control design, Psychiatry Research: Neuroimaging 264 (2017) 60–67. `doi:10.1016/j.pscychresns.2017.04.010`.

[215] D. Lei, W. H. Pinaya, T. van Amelsvoort, M. Marcelis, G. Donohoe, D. O. Mothersill, A. Corvin, M. Gill, S. Vieira, X. Huang, et al., Detecting

schizophrenia at the level of the individual: relative diagnostic value of whole-brain images, connectome-wide functional connectivity and graph-based metrics, Psychological medicine 50 (11) (2020) 1852–1861. `doi: 10.1017/S0033291719001934`.

[216] J. Liu, M. Li, Y. Pan, F.-X. Wu, X. Chen, J. Wang, Classification of schizophrenia based on individual hierarchical brain networks constructed from structural mri images, IEEE transactions on nanobioscience 16 (7) (2017) 600–608. `doi:10.1109/TNB.2017.2751074`.

[217] M. Latha, G. Kavitha, Segmentation and analysis of ventricles in schizophrenic mr brain images using optimal region based energy minimization framework, in: 2017 Fourth International Conference on Signal Processing, Communication and Networking (ICSCN), IEEE, 2017, pp. 1–6. `doi:10.1109/ICSCN.2017.8085735`.

[218] R. Chin, A. X. You, F. Meng, J. Zhou, K. Sim, Recognition of schizophrenia with regularized support vector machine and sequential region of interest selection using structural magnetic resonance imaging, Scientific reports 8 (1) (2018) 1–10. `doi:10.1038/s41598-018-32290-9`.

[219] K. S. Ambrosen, M. W. Skjerbæk, J. Foldager, M. C. Axelsen, N. Bak, L. Arvastson, S. R. Christensen, L. B. Johansen, J. M. Raghava, B. Oranje, et al., A machine-learning framework for robust and reliable prediction of short-and long-term treatment response in initially antipsychotic-naïve schizophrenia patients based on multimodal neuropsychiatric data, Translational psychiatry 10 (1) (2020) 1–13. `doi:10.1038/ s41398-020-00962-8`.

[220] D. Lei, W. H. Pinaya, J. Young, T. van Amelsvoort, M. Marcelis, G. Donohoe, D. O. Mothersill, A. Corvin, S. Vieira, X. Huang, et al., Integrating machining learning and multimodal neuroimaging to detect schizophrenia at the level of the individual, Human brain mapping 41 (5) (2020) 1119–1135. `doi:10.1002/hbm.24863`.

[221] J. Gong, L.-B. Cui, Y.-B. Xi, Y.-S. Zhao, X.-J. Yang, Z.-l. Xu, J.-B. Sun, P. Liu, J. Jia, P. Li, et al., Predicting response to electroconvulsive therapy combined with antipsychotics in schizophrenia using multi-parametric magnetic resonance imaging, Schizophrenia research 216 (2020) 262–271. `doi:10.1016/j.schres.2019.11.046`.

[222] H. Rokham, G. Pearlson, A. Abrol, H. Falakshahi, S. Plis, V. D. Calhoun, Addressing inaccurate nosology in mental health: A multilabel data cleansing approach for detecting label noise from structural magnetic resonance imaging data in mood and psychosis disorders, Biological Psychiatry: Cognitive Neuroscience and Neuroimaging 5 (8) (2020) 819–832. `doi:10.1016/j.bpsc.2020.05.008`.

[223] B. Sutcubasi, S. Z. Metin, T. T. Erguzel, B. Metin, C. Tas, M. K. Arikan, N. Tarhan, Anatomical connectivity changes in bipolar disorder and schizophrenia investigated using whole-brain tract-based spatial statistics and machine learning approaches, Neural Computing and Applications 31 (9) (2019) 4983–4992. `doi:10.1007/s00521-018-03992-y`.

[224] M. Latha, G. Kavitha, Combined metaheuristic algorithm and radiomics strategy for the analysis of neuroanatomical structures in schizophrenia and schizoaffective disorders, IRBM`doi:10.1016/j.irbm.2020.10.006`.

[225] Q. Zhu, H. Li, J. Huang, X. Xu, D. Guan, D. Zhang, Hybrid functional brain network with first-order and second-order information for computer-aided diagnosis of schizophrenia, Frontiers in neuroscience 13 (2019) 603. `doi:10.3389/fnins.2019.00603`.

[226] M. Hu, K. Sim, J. H. Zhou, X. Jiang, C. Guan, Brain mri-based 3d convolutional neural networks for classification of schizophrenia and controls, in: 2020 42nd Annual International Conference of the IEEE Engineering in Medicine & Biology Society (EMBC), IEEE, 2020, pp. 1742–1745. `doi:10.1109/EMBC44109.2020.9176610`.

[227] J. Dakka, P. Bashivan, M. Gheiratmand, I. Rish, S. Jha, R. Greiner, Learning neural markers of schizophrenia disorder using recurrent neural networks, arXiv preprint arXiv:1712.00512.

[228] S. Han, W. Huang, Y. Zhang, J. Zhao, H. Chen, Recognition of early-onset schizophrenia using deep-learning method, in: Applied Informatics, Vol. 4, SpringerOpen, 2017, pp. 1–6. `doi:10.1186/s40535-017-0044-3`.

[229] Y.-W. Niu, Q.-H. Lin, Y. Qiu, L.-D. Kuang, V. D. Calhoun, Sample augmentation for classification of schizophrenia patients and healthy controls using ica of fmri data and convolutional neural networks, in: 2019 Tenth International Conference on Intelligent Control and Information Processing (ICICIP), IEEE, 2019, pp. 297–302. `doi:10.1109/ICICIP47338.2019.9012169`.

[230] W. Yan, S. Plis, V. D. Calhoun, S. Liu, R. Jiang, T.-Z. Jiang, J. Sui, Discriminating schizophrenia from normal controls using resting state functional network connectivity: A deep neural network and layer-wise relevance propagation method, in: 2017 IEEE 27th international workshop on machine learning for signal processing (MLSP), IEEE, 2017, pp. 1–6. `doi:10.1109/MLSP.2017.8168179`.

[231] M. N. I. Qureshi, J. Oh, B. Lee, 3d-cnn based discrimination of schizophrenia using resting-state fmri, Artificial intelligence in medicine 98 (2019) 10–17. `doi:10.1016/j.artmed.2019.06.003`.

[232] W. H. Pinaya, A. Gadelha, O. M. Doyle, C. Noto, A. Zugman, Q. Cordeiro, A. P. Jackowski, R. A. Bressan, J. R. Sato, Using deep belief network modelling to characterize differences in brain morphometry in schizophrenia, Scientific reports 6 (1) (2016) 1–9. `doi:10.1038/srep38897`.

[233] G. Li, D. Han, C. Wang, W. Hu, V. D. Calhoun, Y.-P. Wang, Application of deep canonically correlated sparse autoencoder for the classification of schizophrenia, Computer methods and programs in biomedicine 183 (2020) 105073. `doi:10.1016/j.cmpb.2019.105073`.

[234] K. Oh, W. Kim, G. Shen, Y. Piao, N.-I. Kang, I.-S. Oh, Y. C. Chung, Classification of schizophrenia and normal controls using 3d convolutional neural network and outcome visualization, Schizophrenia research 212 (2019) 186–195. doi:10.1016/j.schres.2019.07.034.

[235] R. Salvador, E. Canales-Rodríguez, A. Guerrero-Pedraza, S. Sarró, D. Tordesillas-Gutiérrez, T. Maristany, B. Crespo-Facorro, P. McKenna, E. Pomarol-Clotet, Multimodal integration of brain images for mri-based diagnosis in schizophrenia, Frontiers in neuroscience 13 (2019) 1203. doi:10.3389/fnins.2019.01203.

[236] W. Yan, V. Calhoun, M. Song, Y. Cui, H. Yan, S. Liu, L. Fan, N. Zuo, Z. Yang, K. Xu, et al., Discriminating schizophrenia using recurrent neural network applied on time courses of multi-site fmri data, EBioMedicine 47 (2019) 543–552. doi:10.1016/j.ebiom.2019.08.023.

[237] J. Oh, B.-L. Oh, K.-U. Lee, J.-H. Chae, K. Yun, Identifying schizophrenia using structural mri with a deep learning algorithm, Frontiers in psychiatry 11 (2020) 16. doi:10.3389/fpsyt.2020.00016.

[238] M. Latha, G. Kavitha, Detection of schizophrenia in brain mr images based on segmented ventricle region and deep belief networks, Neural Computing and Applications 31 (9) (2019) 5195–5206. doi:10.1007/s00521-018-3360-1.

[239] E. Castro, R. D. Hjelm, S. M. Plis, L. Dinh, J. A. Turner, V. D. Calhoun, Deep independence network analysis of structural brain imaging: application to schizophrenia, IEEE transactions on medical imaging 35 (7) (2016) 1729–1740. doi:10.1109/TMI.2016.2527717.

[240] J. Reiter, Developing an interpretable schizophrenia deep learning classifier on fmri and smri using a patient-centered deepshap.

[241] S. M. Plis, M. F. Amin, A. Chekroud, D. Hjelm, E. Damaraju, H. J. Lee, J. R. Bustillo, K. Cho, G. D. Pearlson, V. D. Calhoun, Reading

the (functional) writing on the (structural) wall: Multimodal fusion of brain structure and function via a deep neural network based translation approach reveals novel impairments in schizophrenia, NeuroImage 181 (2018) 734–747. `doi:10.1016/j.neuroimage.2018.07.047`.

[242] L.-L. Zeng, H. Wang, P. Hu, B. Yang, W. Pu, H. Shen, X. Chen, Z. Liu, H. Yin, Q. Tan, et al., Multi-site diagnostic classification of schizophrenia using discriminant deep learning with functional connectivity mri, EBioMedicine 30 (2018) 74–85. `doi:10.1016/j.ebiom.2018.03.017`.

[243] T. Wang, A. Bezerianos, A. Cichocki, J. Li, Multikernel capsule network for schizophrenia identification, IEEE Transactions on Cybernetics`doi:10.1109/TCYB.2020.3035282`.

[244] B. Yang, Y. Chen, Q.-M. Shao, R. Yu, W.-B. Li, G.-Q. Guo, J.-Q. Jiang, L. Pan, Schizophrenia classification using fmri data based on a multiple feature image capsule network ensemble, IEEE Access 7 (2019) 109956–109968. `doi:10.1109/ACCESS.2019.2933550`.

[245] J. Qi, J. Tejedor, Deep multi-view representation learning for multimodal features of the schizophrenia and schizo-affective disorder, in: 2016 IEEE International Conference on Acoustics, Speech and Signal Processing (ICASSP), IEEE, 2016, pp. 952–956. `doi:10.1109/ICASSP.2016.7471816`.

[246] G. Li, C. Wang, D.-P. Han, Y.-P. Zhang, P. Peng, V. D. Calhoun, Y.-P. Wang, Deep principal correlated auto-encoders with application to imaging and genomics data integration, IEEE Access 8 (2020) 20093–20107. `doi:10.1109/ACCESS.2020.2968634`.

[247] A. Zhou, Y. Cui, T. Jiang, Multisite schizophrenia classification based on brainnetome atlas by deep learning, in: 2018 5th IEEE International Conference on Cloud Computing and Intelligence Systems (CCIS), IEEE, 2018, pp. 451–455. `doi:10.1109/CCIS.2018.8691336`.

[248] S. Srinivasagopalan, J. Barry, V. Gurupur, S. Thankachan, A deep learning approach for diagnosing schizophrenic patients, Journal of Experimental & Theoretical Artificial Intelligence 31 (6) (2019) 803–816. `doi:10.1080/0952813X.2018.1563636`.

[249] P. Patel, P. Aggarwal, A. Gupta, Classification of schizophrenia versus normal subjects using deep learning, in: Proceedings of the Tenth Indian Conference on Computer Vision, Graphics and Image Processing, 2016, pp. 1–6. `doi:10.1145/3009977.3010050`.

[250] Y. Zhu, S. Fu, S. Yang, P. Liang, Y. Tan, Weighted deep forest for schizophrenia data classification, IEEE Access 8 (2020) 62698–62705. `doi:10.1109/ACCESS.2020.2983317`.

[251] J. Kim, V. D. Calhoun, E. Shim, J.-H. Lee, Deep neural network with weight sparsity control and pre-training extracts hierarchical features and enhances classification performance: Evidence from whole-brain resting-state functional connectivity patterns of schizophrenia, Neuroimage 124 (2016) 127–146. `doi:10.1016/j.neuroimage.2015.05.018`.

[252] T. Matsubara, T. Tashiro, K. Uehara, Deep neural generative model of functional mri images for psychiatric disorder diagnosis, IEEE Transactions on Biomedical Engineering 66 (10) (2019) 2768–2779. `doi:10.1109/TBME.2019.2895663`.

[253] Z. Wang, Y. Sun, Q. Shen, L. Cao, Dilated 3d convolutional neural networks for brain mri data classification, IEEE Access 7 (2019) 134388–134398. `doi:10.1109/ACCESS.2019.2941912`.

[254] Y. Hashimoto, Y. Ogata, M. Honda, Y. Yamashita, Deep feature extraction for resting-state functional mri by self-supervised learning and application to schizophrenia diagnosis, bioRxiv`doi:10.1101/2020.08.22.260406`.

[255] J. Zhao, J. Huang, D. Zhi, W. Yan, X. Ma, X. Yang, X. Li, Q. Ke, T. Jiang, V. D. Calhoun, et al., Functional network connectivity (fnc)-based generative adversarial network (gan) and its applications in classification of mental disorders, Journal of neuroscience methods 341 (2020) 108756. `doi:10.1016/j.jneumeth.2020.108756`.

[256] H. Yamaguchi, Y. Hashimoto, G. Sugihara, J. Miyata, T. Murai, H. Takahashi, M. Honda, A. Hishimoto, Y. Yamashita, Three-dimensional convolutional autoencoder extracts features of structural brain images with a diagnostic label-free approach: Application to schizophrenia datasets, bioRxiv`doi:10.1101/2020.08.24.213447`.

[257] S. Campese, I. Lauriola, C. Scarpazza, G. Sartori, F. Aiolli, Psychiatric disorders classification with 3d convolutional neural networks, in: INNS Big Data and Deep Learning Conference, Springer, 2019, pp. 48–57. `doi: 10.1007/978-3-030-16841-4_6`.

[258] H. Nguyen, R. W. Morris, A. W. Harris, M. S. Korgoankar, F. Ramos, Correcting differences in multi-site neuroimaging data using generative adversarial networks, arXiv preprint arXiv:1803.09375.

[259] S. M. Smith, Overview of fmri analysis, The British Journal of Radiology 77 (suppl_2) (2004) S167–S175. `doi:10.1259/bjr/33553595`.

[260] S. M. Smith, Bet: Brain extraction tool, FMRIB TR00SMS2b, Oxford Centre for Functional Magnetic Resonance Imaging of the Brain), Department of Clinical Neurology, Oxford University, John Radcliffe Hospital, Headington, UK.

[261] D. Librenza-Garcia, B. J. Kotzian, J. Yang, B. Mwangi, B. Cao, L. N. P. Lima, M. B. Bermudez, M. V. Boeira, F. Kapczinski, I. C. Passos, The impact of machine learning techniques in the study of bipolar disorder: a systematic review, Neuroscience & Biobehavioral Reviews 80 (2017) 538–554. `doi:10.1016/j.neubiorev.2017.07.004`.

[262] Z. Mao, Y. Su, G. Xu, X. Wang, Y. Huang, W. Yue, L. Sun, N. Xiong, Spatio-temporal deep learning method for adhd fmri classification, Information Sciences 499 (2019) 1–11. `doi:10.1016/j.ins.2019.05.043`.

[263] X. Yi, E. Walia, P. Babyn, Generative adversarial network in medical imaging: A review, Medical image analysis 58 (2019) 101552. `doi:10.1016/j.media.2019.101552`.

[264] J. Gui, Z. Sun, Y. Wen, D. Tao, J. Ye, A review on generative adversarial networks: Algorithms, theory, and applications, arXiv preprint arXiv:2001.06937.

[265] W. Wang, V. W. Zheng, H. Yu, C. Miao, A survey of zero-shot learning: Settings, methods, and applications, ACM Transactions on Intelligent Systems and Technology (TIST) 10 (2) (2019) 1–37. `doi:10.1145/3293318`.

[266] Y. Xian, T. Lorenz, B. Schiele, Z. Akata, Feature generating networks for zero-shot learning, in: Proceedings of the IEEE conference on computer vision and pattern recognition, 2018, pp. 5542–5551.